Energy & Environmental Science

Accepted Manuscript

ROYAL SOCIETY OF CHEMISTRY

www.rsc.org/ees

A perspective on the production of dye-sensitized solar modules

Azhar Fakharuddin[a], Rajan Jose[*a], Thomas M. Brown[b], Francisco Fabregat-Santiago[c], Juan Bisquert[*c,d]

[a]*Nanostructured Renewable Energy Materials Laboratory, Faculty of Industrial Sciences & Technology, Universiti Malaysia Pahang, 26300, Malaysia*
[b] *C.H.O.S.E. (Centre for Hybrid and Organic Solar Energy), Department of Electronic Engineering, University of Rome–Tor Vergata, via del Politecnico 1, 00133, Rome, Italy*
[c]*Photovoltaic and Optoelectronic Devices Group, Departament de Física, Universitat Jaume I, 12071 Castelló, Spain*
[d]*Department of Chemistry, Faculty of Science, King Abdulaziz University, Jeddah, Saudi Arabia*

Abstract

Dye-sensitized solar cells (DSCs) are well researched globally due to their potential to be a low-cost photovoltaic (PV) device, especially suited for building and automobile integrated PV (BIPV, AIPV) and portable or indoor light harvesting applications. Large monetary and intellectual investments for developing them into a deployable technology created a wealth of knowledge on nano-interfaces and devices through an increasing numbers of research reports since 1991. In response to those investments, the dawn of the new millennium witnessed the emergence of a corporate sector on DSCs. Advances in their device designs, their incorporation on flexible substrates, development of solid state modules, enhanced stability under outdoor exposure, and the advancements in their scalable fabrication tools and techniques elevated the DSCs from laboratory to real-life applications. Although photoconversion efficiencies are not on par with commercially available CIGS or single crystalline silicon solar cells, the features of transparency, light weight, flexibility, conformability, workability under low-light conditions, and easy integration in buildings as

solar windows compel further dwelling in DSC modules. In fact DSC panels have been shown to deliver even more electricity compared to the silicon and the thin film counterparts of similar power rating when exposed to low light operating conditions, due to their workability at such conditions, thereby offering possibilities to be market leaders in BIPV and indoor light harvesting photovoltaic technology. However, the large area dye-solar modules lacks in performance compared to their laboratory scale devices and also suffer from long term stability issues. Herein, we discuss the main factors behind their inferior photovoltaic performance and also identify the opportunities in materials' architecture and device designs for more efficient DSC modules.

Keywords: Renewable energy, Organic photovoltaics, roadmap of dye solar cells, solar module designs, charge transport in dye solar modules.

1. Introduction—renewable energy scenario

Primary supply of clean and sustainable energy is one of the top global issues. A greater portion of today's energy demand (>85%) is fulfilled by fossil fuel based resources but at the expense of the global warming and consequent severe impact on climate changes.[1] The statistics of increasing energy demand and depleting fossil fuels are alarming: (i) the energy demand is expected to increase 2 folds by 2050; and (ii) due to depleting fossil fuel reserves an additional energy demand equal to today's total energy consumption is expected in next three decades.[2, 3] The renewable energy resources such as solar and wind are potentially cost effective, abundant in nature, and are fairly distributed across the globe, therefore, have potential to contribute towards this energy gap.[4] These resources also eliminate the environment issues associated with the use of fossil fuels. Among the renewable energy resources, solar energy alone has the potential to meet world's primary energy demand; it requires covering less than 0.4% of our planet's surface with 15% efficient solar

panels.[5] Alternatively, using 25% efficient solar panels, a solar farm of area ~400 km × 400 km in the Sahara desert would meet the projected energy demand. Above all, energy from sunlight is 200 times more abundant than all other renewable energy resources combined.[3]

Photovoltaic effect was discovered in the 19th century by Edmond Becquerel. Subsequently, solar energy appears not only as a promising alternative energy resource but also a better off–grid choice in remote applications and in portable electronics. The solar cell technology can be divided into three types, (i) crystalline silicon solar cells, (ii) thin film solar cells ($CuInGaSe_2$, CdTe, a-Si:H etc.) called thin as their working electrode comprises of much thinner films (~1 μm) compared to that of the first generation (~350 μm), and (iii) molecular absorber solar cells in which molecules or inorganic clusters are the primary absorbers. Examples of the last type are polymer solar cells, dye-sensitized solar cells (DSCs), quantum dot solar cells, and recently emerged perovskite solar cells. Over half a century research in silicon based solar cells, which currently dominate the photovoltaic market, resulted in an installed capacity of >40 GW till date, up from 1.5 GW in 2000 as shown in Figure 1.[6] This installation brought solar cells (mostly silicon based) to contribute to energy demand in peak hours; in Germany ~5.3% of daily demand is fulfilled by solar electricity which increases to 20% in longer sunny days.[4,7] Commercial modules of silicon based solar cells (first generation) of efficiency (η) up to ~20% are routinely available in the market. On the other hand, thin film solar cells (second generation) based on $CuInGaSe_2$ (CIGS) have achieved η >20% at laboratory scale;[8,9] and commercial modules of η ~15% are available in the market.[10] Despite the rapidly increasing global installations, many of the first and second generation solar cells still suffer from issues such as long payback, relatively high costs associated with extreme purity requirement in the active material, scarcity of materials such as indium and silver, their low working capability in cloudy hours or in shaded regions.[4, 11] Besides, owning to their opacity (for example, silicon solar cells), these solar

cells are not a choice for integration in buildings. These drawbacks bring into account the third generation photovoltaics, which aims to resolve many of the issues of the first two generations. Although initial developments for these new photovoltaics entail delivering applications, building integrated photovoltaics (BIPV), automotive integrated photovoltaics (AIPV) for example, their further cost reduction remains an important target as the cost of silicon solar cells is seen to be significantly dropped in recent years. However, the third generation devices currently generally suffer from lower η and short term outdoor stability compared to the other two well-established photovoltaics.

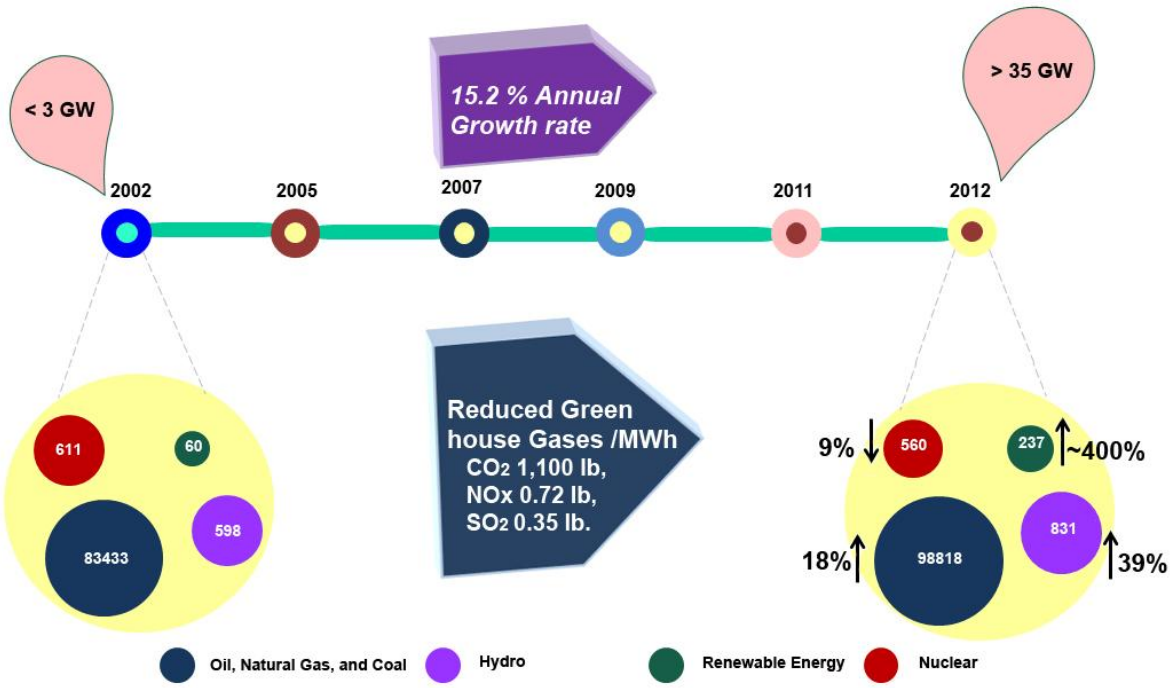

Figure 1: (a) A chart showing paradigm shift of the share of renewable energy sources (data collected from ref.[12] and ref.[13]). The values are in million tons of oil equivalents (mtoe).

Purpose of this article is to review the progress made in deploying a third generation solar cell – the dye sensitized solar cell (DSC) – from the laboratory scale to the real life application. Comparable photoconversion efficiency with that of market leading CIGS or single crystalline silicon solar cells is yet to be achieved by DSCs; however, positive inherent features as their workability under low-light conditions, transparency, flexibility,

conformability, superior performance under low levels or indoor light conditions and easy integration in buildings as solar windows will facilitate their market entry. This article is organized as follows: section 2 outlines the working principle, various components and types of laboratory scale DSCs. Section 3 of this article compares the outstanding features of DSC technology that facilitates its entry into photovoltaic market. In section 4, we discuss their worldwide business growth and in sections 5 – 9, the developments in dye–solar modules (DSMs) are elaborated. Section 10 critically analyze the major factors behind the areas of inferior performance of DSMs and also introduces alternative designs of these modules. Research in long term stability of DSMs is reviewed in section 11 while section 12 talks about the standards required for elevating DSCs from laboratory to a successful commercial application. In Section 13, we conclude our observations and make recommendations to open up windows for future research for high performance and cost effective DSMs.

2. Dye-sensitized solar cells

Among various types of 3rd generation solar cells, DSCs are promising as they are cost effective, relatively easier to fabricate on large panels, light weight and flexible, and offer transparency compared to the first two generation solar cells.[14-16] Due to the unique feature of transparency,[17] DSCs can easily be integrated into BIPVs and in AIPVs, however, the outdoor long term stability is yet to be achieved. Furthermore, they have shown superior performance under indoor lighting[18] and also been developed extensively on flexible substrates.[19] Many reports are published on the phenomenology of photovoltaic action in DSCs and choice of various materials used.[20-22] The DSC is a photoelectrochemical device in which the photocurrent is generated at a junction between a dye-anchored metal oxide semiconductor and a hole-conducting electrolyte upon light absorption. Various materials and

their interfaces constituting the DSCs and the photochemical process are explained in the Figure 2.

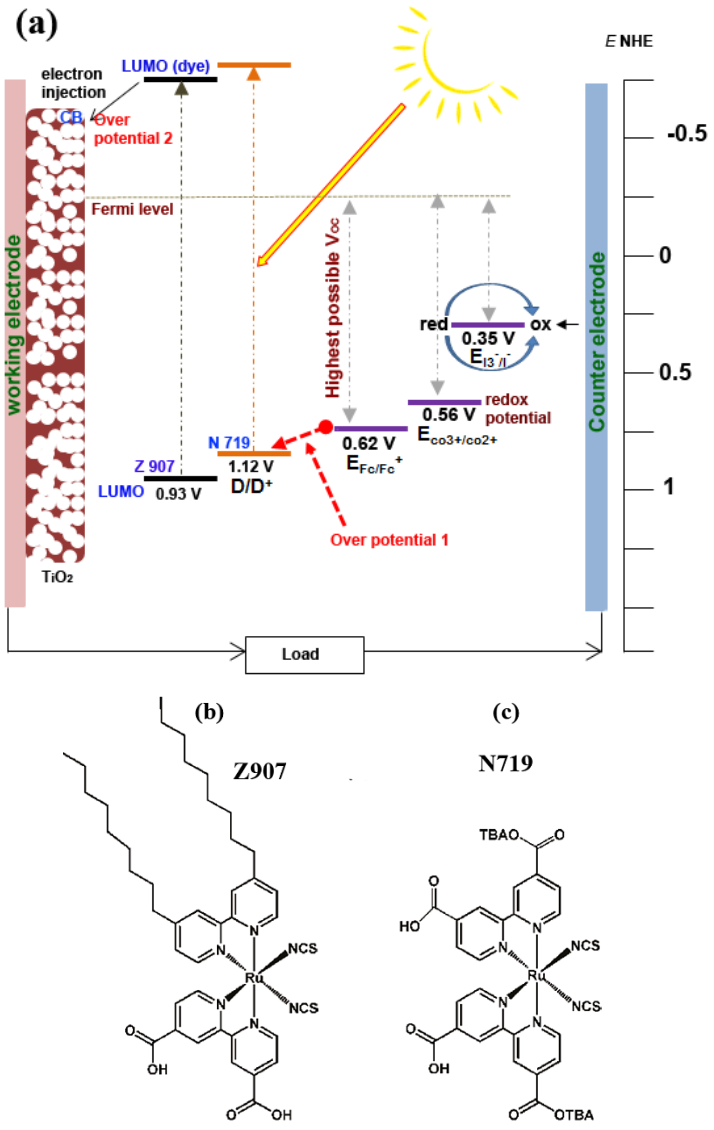

Figure 2: Schematics of the working mechanism of a DSC. N719 and Z907 are Ruthenium based dyes. E_{CO}^{3+}, $E_{Fc/Fc}^{+}$, and $E_{I3}^{-}/_{I}^{-}$ are the electrochemical potentials of the cobalt, ferrocene and iodide electrolytes, respectively measured with respect to a standard hydrogen electrode (NHE). The working electrode (WE) is a mesoporous film of thickness ~3 – 20 μm of a metal oxide semiconductor (MOS, usually TiO_2) is coated on a conducting glass substrate. The film is then conjugated with a molecular absorber (dye); a junction is made by putting the film in contact with an electrolyte and subsequently sealed with a conducting counter electrode (CE) equipped with a catalyst layer. Upon absorption of sunlight, the dye oxidizes and injects the photogenerated electrons into the MOS which are collected at the WE. The oxidized dye is regenerated by accepting electrons from the redox couple. The electron travels to the CE via an external circuit and completes the cycle. Fractions of absorbed energy are lost at the dye-TiO_2 interface (overpotential#1) and the dye-electrolyte interface (overpotential#2).

The rest i.e. {absorbed energy – (overpotential #1+overpotential #2)} contribute to the open circuit voltage (V_{OC}). The redox potentials and HOMO level of the dyes are taken from the references 23,24 and figure b & c are the chemical structures of the dyes Z907 and N719, respectively. Figures adapted from reference 25 with permission from American Chemical Society.

DSCs are promising due to their low cost fabrication compared to the first two generation solar cells; however, their η is much lower than commercially available thin film and silicon solar modules. Although η up to ~13% was reported in DSCs[26] the certified value is ~11.9% for devices built on rigid substrates (fluorine doped tin oxide (FTO) coated glass)[9] and ~7.6% built on flexible substrates (Polyethylene terephthalate (PET)/indium tin oxide (ITO)).[27] As shown in Figure 3, independent certifications for other types of DSCs such as solid state DSCs (*s*-DSCs), p-type DSCs (*p*-DSCs), and tandem DSCs (*T*-DSCs) are yet to be seen. In view of commercial applications, solar panels outdoor stability is crucial besides their η. For example, amorphous silicon (~10%) and organic thin film modules (6.8%) with η much lower than the certified value of DSMs (8.2%) are available in the market owing to their significantly higher lifetime (~ 20 years for thin film modules).[28] Although DSCs have shown significant stability in indoor accelerated testing[29, 30] the lifetime of liquid electrolyte based DSCs (*l*-DSCs) is far lower in outdoor conditions due to their high volatility. Alternatively, *s*-DSCs have been developed in order to overcome some of the issues related to the liquid electrolyte. Future research on *s*-DSCs to be dedicated to solve their primary issues such as poor pore filling (infiltration of hole transport material into mesoporous MOS), inferior hole mobility and hole diffusion length in these devices. The *T*-DSCs are also promising; however, their performance is limited due to the low voltage of *p*-type photocathodes.[31]A breakthrough in the third generation solar cells is the emergence of perovskite sensitized solid state solar cells (PSCs) which employ an organic – inorganic hybrid perovskite absorber (commonly $CH_3NH_3PbX_3$, X = Br, Cl, or I) on a very thin MOS

layer (< 1μm),[32-37] Although PSCs initially emerged as a class of DSCs, they are likely to be considered a new class of solar cells. The confirmed η as high as ~17.9% was reported in PSCs which is a four times increment in just four years since its first report.[9] The PSCs, which are recently at their spring, are another emerging area; nevertheless, the replacement of lead (Pb) with some non-toxic material may presumably increase its market acceptability.[38] Results on the scalable fabrication of PCSs have recently been reported across the globe with η up to 8.7%.[39, 40]

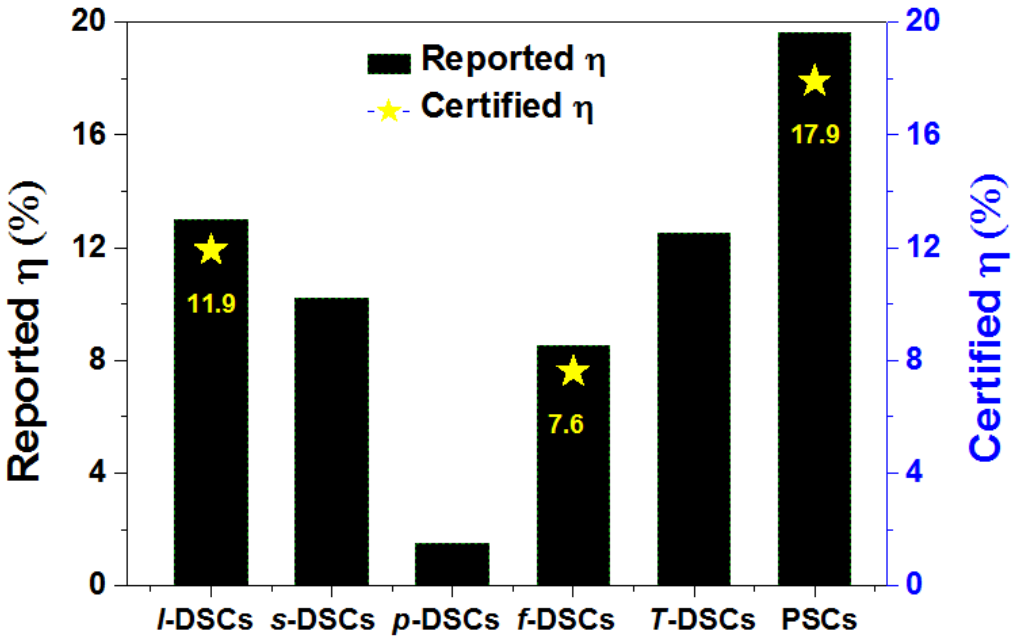

Figure 3: Efficiency comparison of various types of DSCs. The stars show certified efficiency values of corresponding devices. The confirmed η for various devices is reported in reference [9].

3. DSCs versus other PV technologies

One of the major drawbacks of the conventional silicon PV technology is the amount of solar irradiation required for its start-up operation (200-300 watt/m^2) which increases to 800-900 watt/m^2 for peak performance.[41] Despite the fact that the certified η in DSMs (8.2%)[76] are far lower than that is achieved in the first two generation solar cells (~15 – 20%), their

working capability in low light conditions and transparency place them at the forefront for applications such as BIPVs. This exclusive feature of DSMs not only increases their operating hours but also deploys them in shaded regions, corners or bends in buildings. A comparative study by Dyesol Ltd. revealed that DSMs delivers 65-300% higher power output in cloudy days compared to silicon and thin film solar cells as shown in Figures 4(a&b).[42] Their analysis revealed that the performance of DSMs is higher in days when the solar irradiance is <300 kW/m^2. In another six month comparative study by Aisin Seiki CO. Ltd., [43] DSMs (64 cell modules of size 10 × 10 cm^2) showed 10% increased performance in a hot sunny day and 20% higher in a cloudy day than single crystalline Si-modules. The study also showed better performance of DSMs in midmorning and midevening thus widening the available performing hours. A similar performance was demonstrated in Japan in a world solar car rally (July 2008), where a 2×8 m^2 DSMs (developed by Taiyo Yuden Co. Ltd.) were deployed on a test race car and achieved a speed of 11.8 km/h in cloudy weather which was almost similar to 12.5 km/h in sunny weather.[43] These reports spotlight the exclusive features of DSMs and their capability of working in low light conditions that overcome the limitations of the conventional PV technology. Moreover, a recent study by Zardetto *et al*.[44] showed that DSMs on flexible substrates when turned into a curve shape outperform a flat device thereby further strengthens the claim on their application diversity. The study showed ~10% higher power output in the flexible device built on a metallic substrate than a flat one when normalized to their footprint. All these results are encouraging for DSMs' potential applications at low light areas and conditions. As an example, in zero energy buildings DSMs can be deployed as smart windows to simultaneously add aesthetic while producing solar electricity almost entire day.

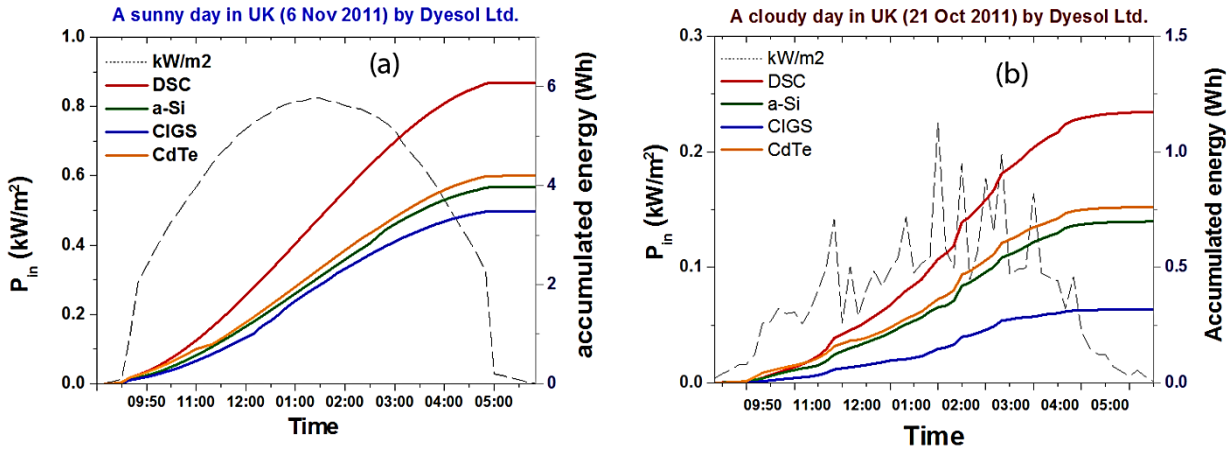

Figure 4(a): Performance comparison of DSCs' with other photovoltaic technologies on a sunny day, (b) a cloudy day (data courtesy to Dr. Damion Milliken of Dyesol Ltd.).

Unlike the first two generation solar cells, which require clean room and vacuum based device fabrication facilities, DSMs can be fabricated in less demanding conditions. To further ease its fabrication, researchers successfully showed low temperature (<150 °C) binder free coating process on plastic substrates and demonstrated η as high as ~8% in their single cells[27] and ~3-4.5% % in DSMs.[45,46]

The performance of DSCs improves from room temperature to ~40 °C[47] because viscosity of the electrolyte decreases upon increase in temperature which meliorates the ionic transport inside the MOS.[48, 49] Conversely, silicon based solar cells drops in performance at elevated temperatures as the dark recombination current increases with temperature.[50, 51]

3.1 Manufacturing cost for DSMs

Besides the advantage of DSMs for applications in low-light and flexible conditions, its deployability would strongly depend on the module manufacturing cost and associated economics. Table 1 shows a comparison of manufacturing cost normalized with respect to the peak output power compiled from various sources. Kalowekamo *et al.*[52] estimated the manufacturing cost for DSMs and compared it with first two generation solar cells. In their

study, the estimated DSM cost varies from 0.5\$/W_P (η ~5%) – 1\$/W_P (η ~15%). The DSMs provide solar electricity at a cost significantly cheaper than first two generation of solar cells (Table 1). A DSM manufacturer Fujikura Ltd. reports that the manufacturing cost can be reduced to 0.4\$/W_P provided an annual production level of 100 MW is achieved.[53] Lower cost of DSMs could be attributed to the cheaper material cost and easy fabrication. Besides, the photoelectrode MOS such as TiO_2, ZnO, SnO_2, are largely abundant unlike indium which is a used in come of the thin film solar cells .[4]

Table 1: Cost/W_P and η comparison of various types of solar cells/modules; the values are taken from ref. ([28]) unless stated otherwise. Certified efficiencies are marked with a '*'

*Market prices of silicon panels have droped in latest years to as low as ~0.7 \$/Wp; however, such prices are from few producers and the realisticity and sustainability of such prices are yet to be determined. (http://www.nyse.com).

Device	η in cells (%)	η in modules (%)	Module manufacturing cost/W_p(\$)
Multijunction (III– V)	44.7* (FhG-ISE)	---	---
Si	24.7 (UNSW)	14.5 (ref. [54])	~0.7*-1.29 (ref. [55])
CIGS	19.8* (NREL)	18.7*(FhG-ISE)	1.13 (ref.[55])
Si (amorphous)	10.1* (AIST)	---	---
CdTe	17.3* (NREL, ref.[55])	11.7	0.74
Organic PVs	10 (ref. [55])	6.8*	0.75-2 (ref. [56])
Dye solar cells	11.9* (SHARP)	8.2* (SHARP)	0.5-0.94(ref[52,57])
Perovskite solar cells	17.9*[9]	8.7 (planar structure)%[40] 5.1% (Monolithic modules)[39]	NA
QDSCs	7(ref.[58])	Not developed yet	NA

Major contribution (50 – 60%) to DSMs' manufacturing cost arises primarily from dyes, electrolyte, and substrates.[57,59] Furthermore, the materials for DSMs are still produced on research scale; the cost would significantly reduce on a commercial scale production.

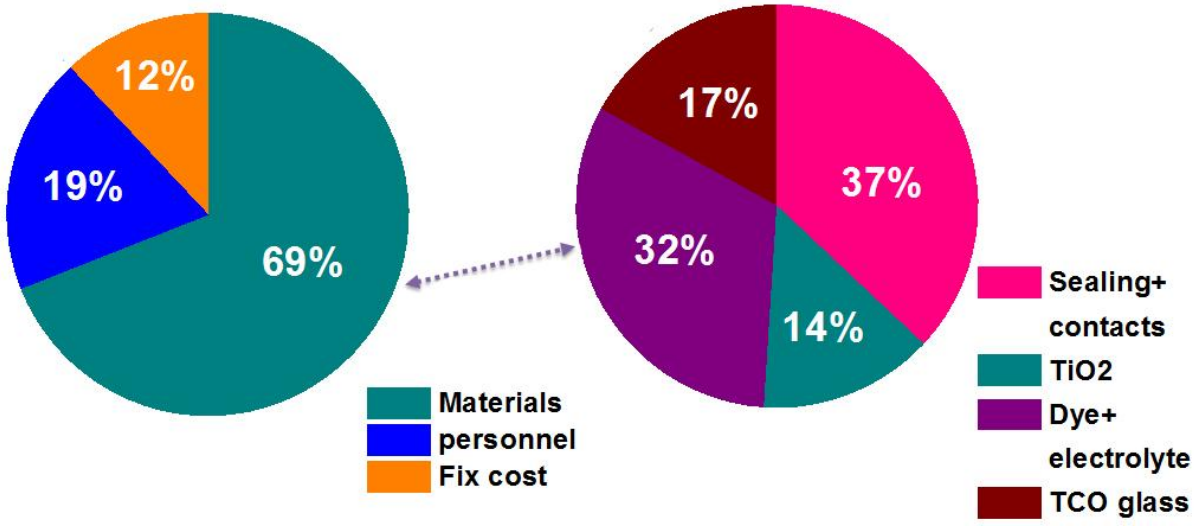

Figure 5: Left panel is estimation of the projected share to overall cost during large scale manufacturing and the right panel is cost for various materials while fabricating the 20 MW DSMs. Data taken from reference[59].

Figure 5 shows manufacturing cost data for series monolithic DSMs (90 cm ×60 cm, power output 50 W_P/m^2). These statistics were compiled by one of the world leading DSM developers, Solaronix Ltd., for an annual production of ~20 MW_P/year.[59]The DSMs manufacturing cost was estimated to be ~0.97 Euro/W_P with η ~7% and ~90% process output yield. Notably, two thirds of the total cost arise from materials where dyes and electrolytes contribute one third, sealing and interconnections cost more than one third (37%) and substrates cost ~17% of the material cost (~22%, ~25% and ~12% of the total cost, respectively). As suggested by Hashmi *et al.*[57] a substantial decrement of this price is possible by replacing some of the expensive material components; i.e., replacing glass with plastic will reduce substrates cost by one third, although one must consider the additional costs of additional barrier layers. Replacing FTO by stainless steel sheets can save up to 80% of the substrate cost (9% of the total cost). Similarly, although *s*-DSCs offer less sealing difficulties than *l*-DSCs however, they are still vulnerable to moisture and oxygen permeation.

4. Dye-solar modules: From laboratory to commercial development

After the η report in 1991 of single cells, the same group reported first DSMs in the year 1996.[60] In their module, six DSCs of area ~3.3 cm^2 were serially connected on an FTO substrate to get η ~5.3%. Since then a number of reports have been published across the globe for the development of various type of DSMs in various designs including series, parallel or their combination. A survey of literature shows that efforts in the development of DSMs are rather unimpressive: only one research paper is published for DSMs for each hundred papers on laboratory devices. Figure 6 (a) shows a summary of research papers and patents published on DSCs and DSMs. A study on the country's involvement in DSMs are also made and shown in Figure 6(b). One would observe that China, Japan, Korea, Taiwan and the USA are the leaders in DSM fabrication in the descending order of their contribution.

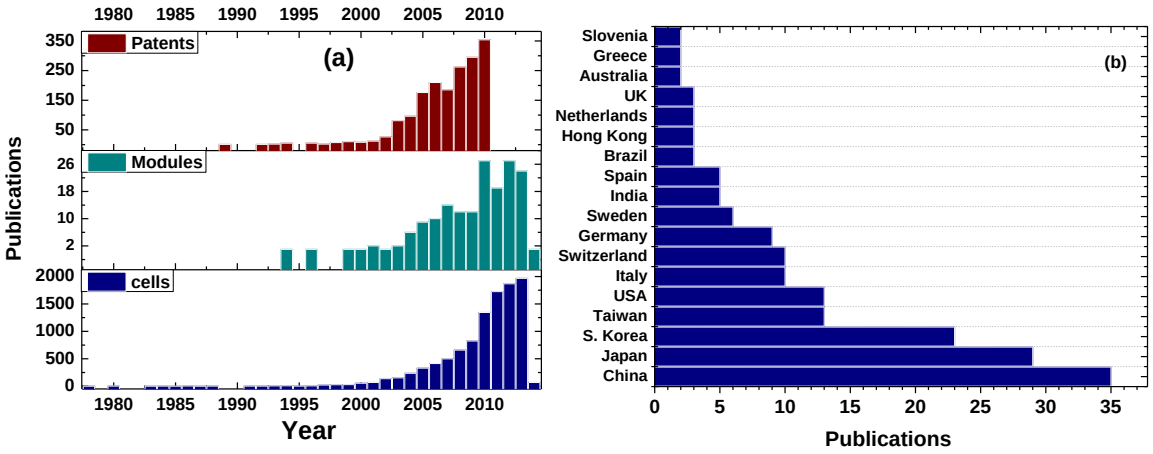

Figure 6(a): Research trends in DSCs, (i) bottom panel indicates papers published on single cells, (ii) middle panel represents publications on DSMs, and (iii) patents registered globally (data is taken from reference [61]), and **(b)** trends shows the affiliation of various countries working on large area development of DSCs. (Data is taken from Scopus on January 2014 using keywords 'dye-sensitized solar modules' and 'large area dye-sensitized solar cells').

4.1 Dye-solar cell/modules as electrochromic windows

For residential and commercial users, a significant portion (10-30%) of the peak electricity demand arises from overheating caused by glass windows that allows heat radiation to enter into a building.[62] This share can be reduced by (i) controlling the optical transparency of the windows to block heat radiations entering the buildings and (ii) converting the passive windows into smart windows that can additionally harvest the solar light into electricity.[63-65] Towards the second strategy, an energy storage smart window, also called electrochromic device (ECD), that simultaneously harvest and store the solar energy by integrating two electrochemical devices (DSC and supercapacitors) has been developed.[66, 67] The ECD can be divided into two parts, photovoltaic and EC components separated by an ionic conductor with negligible electronic conductivity to avoid short circuit between them. Such devices are self-powered unlike the conventional ECD windows which need an energy supply for its operation. The window changes from bleached to colored state due to the reversible reaction in the electrolyte upon light absorption.[68]

Self-powered switchable devices can be made in two ways: (i) photoelectrochromic window (PECW), which changes its transmittance using electrical output of the DSC and thereby blocks heat radiations (Figure 7)[69]and (ii) smart energy storage window where prime concern is to produce electricity and store it in an integrated supercapacitor.[66] The primary requirement for PECWs is an electrochemical material which changes its transmittance with an applied potential. Various metal oxides (WO_3, NiO, IrO_2, and Nb_2O_5) and polymers such as polyaniline and Poly(3,4-ethylene-dioxythiophene) have been employed as an EC material.[70-73] In a recent study, Yang *et al*.[69] reported a lowering of transmittance from 47 to 9% upon electrochemical reaction employing PECW (η ~1.2%). In another report, Al doped boron oxide based PECW reported η up to ~2% owing to conductivity of the dopant used.[74]

Figure 7: Switching sequence of an ECW. Figure adapted from reference [75].

As the self-powered switchable devices need to be highly transparent, the films should be made very thin. These devices usually consist of three sequentially coated layers and required precise fabrication to avoid short circuit.[76,77] Thin silicon solar modules are commercially available as a switchable windows with η ~5%;[78] however, DSC based ECDs are still in the laboratory stage. There are rare reports on employing *T*-DSCs as switchable or smart windows; however, the work is still at laboratory scale.[79]

4.2 Emergence of dye solar modules business

DSMs have now reached a level of deployment as a photovoltaic device. Table 2 shows a list of industrial sectors that have emerged develpoing this photovoltaic technology, their inferred core business and key achievements. Owing to the transparency in DSCs and their excellent performance in low level of light illumination, the potential key venues for installing DSCs are indoor electronic application and BIPV (Figure 8 a – d),[80] as its efficiency vs transparency performance can be tuned.[17] DSCs work well in diffused or low light and is less effected by the angle of incidence with efficiencies which increase with angle of light incidence (up to ~50^{o}) by ~10–16%%.[81] Moreover, BIPVs has the advantage over centralized solar power generation represented by the fact that electricity generated is consumed at the same place thereby avoiding the transmission line losses and infrastructure cost. DSMs with

active area of ~200 m^2 were installed as windows of a green building in April 2014 at the École Polytechnique Fédérale De Lausanne (EFPL) campus, Switzerland (Figure 8a & b).[82] These panels are estimated to be able to generate ~2000 kWh of annual solar electricity. These transparent panels are in five different colors (representing a desirable unique feature of DSCs) and were developed by Solaronix. This massive production is an important milestone for the commercial deployment of DSCs although a number of issues including lifetime of these panels under operating conditions for many are yet to be fully addressed.

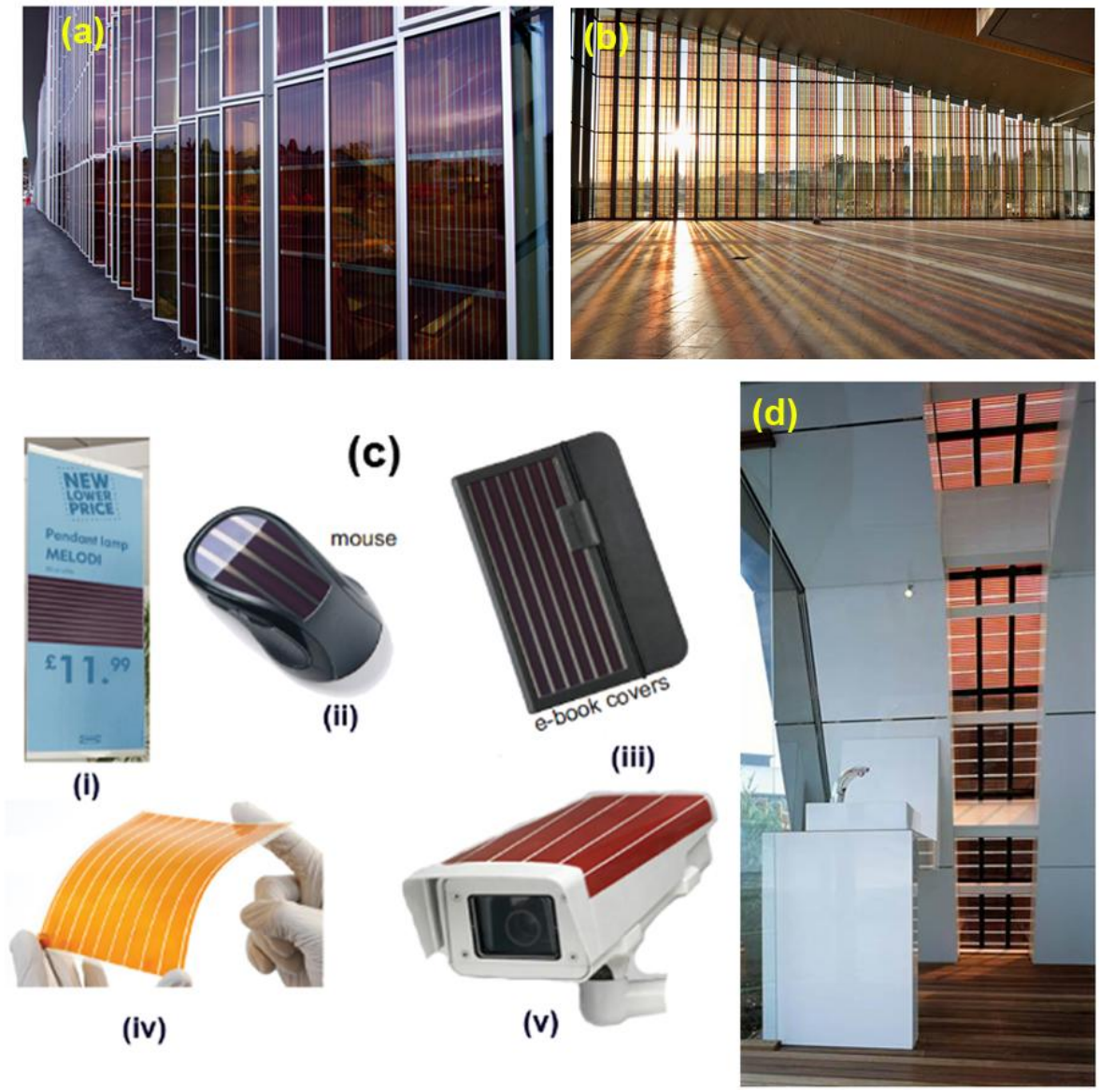

Figure 8: (a & b) DSMs installation recently completed at EFPL campus (Photos are courtesy of David Martineau of Solaronix Ltd.), and **(c)** images of few commercial DSC products in market (i—iii are

indoor electronics by G24 and iv and v are developed by 3G Solar., and **(d)** DSMs installed as an interior of a washroom by Dyesol Ltd. (Image courtesy: Dr. Damion Milliken of Dyesol Ltd.).

Dyesol, another leading industry in DSCs, has recently launched projects on the integration of DSCs into buildings with their various industrial partners (Tata Steel Europe of UK, Pilkington North America of USA, Timo Technologies of South Korea), and on DSC powered Combined Energy Generation and Storage (CEGS) devices.[83] These projects are expected to further reduce the cost/kWh as double coated glass windows in the buildings, meant for UV protection and antireflective coatings, are used as substrates for DSMs. Oxford Photovoltaics, a spin-off company of Oxford University, is working on all solid state perovskite based modules (PSMs). However, the lifetime of the solid state PSMs under outdoor conditions is yet to be realized.

Table 2: Globally emerged commercial companies on dye-solar cells/modules developments. The information is inferred from their websites/published reports on websites and (ref [43]), unless stated otherwise.

No	Company	Affiliation	Core Business	Major Achievements in DSCs
1	S Samsung SDI	Korea	Electronic devices such as LCDs, mobile phones, and more recently energy storage and harvesting devices	Dye solar panels for BIPVs, smart windows with integrated storage, tandems DSPs.
2	SHARP	Japan	Electronic products	Certified η of 11.9% in single cells by tuning haze effect, certified highest module PCE (8.2 %) in W-type module, cost effective back contact DSCs (η ~7.1%) with only one substrate, 8.1% efficient quasi *s*-DSCs employing a polymer electrolyte.
3	G24 Power	UK	Solar power especially third generation PVs	Started DSC plant in 2007 (18000 sq. ft), flexible water proof bags, commercial application for indoor electronics, roll-to-roll processing capability of 800m in ~ 3hrs, specialized in indoor electronics such as key-boards, mouse, e-book cover, solar bags, MP3 etc.
4	Konarka	USA	Spinout company of MIT for DSCs	Licensed it DSC IP to G24.
5	Dyesol	Australia	DSCs materials and commercial development	DSMs, BIPVs, Integration of DSCs in roof material (in process), *s*-DSMs and *f*-DSMs. Developing DSMs and *s*-DSMs.
6	Solaronix	Switzerland	DSCs materials and commercial development	Panels of an active area ~200m^2 are shipped for EFPL with an estimated annual production of 2000kWh. Developing DSMs and materials for solar cells/modules.
7	Dynamo	Sweden	DSCs materials and commercial development	Preparing Co-based electrolytes and Porphyrine dyes.
8	Oxford PVs	UK	*s*-DSMs, PSMs	Currently working on perovkite solar modules.

9	Dyepower	Italy	Development of DSM for BIPV and facades applications	Running an automated pilot line for the production of A4 size DSMs and for larger area strings/panels. UV, humidity-freeze and damp-heat IEC 61646 stability tests successfully passed on A4 size modules.
10	EFPL	Switzerland	Organic PVs, materials and characterization	Held the main patent on mesoporous dye solar cells structure. Highest uncertified η in DSCs (13%), one of the highest η in perovskite based solar cells (15%), the first report on DSMs in 1996 (monolithic series modules (10×10 cm^2) with η ~ 6%.
11	Fujikura	Japan	Optical fibers	Developing DSCs for both outdoor applications and indoor electronics such as mobile phones, testing ionic liquids and gel-electrolytes in modules, thermal stability and outdoor testing of more than 200 sub modules (20 cm^2) modules passed IEC 61646 (stability test).
12	3G Solar	Israel	DSCs technology	Installed DSC mini modules to charge computer peripherals, surveillance cameras, electronic bracelets and medical devices.
13	CSIRO	Australia	Research agency	Colorful and transparent DSMs for BIPVs, materials for cost-effective DSCs.
14	Taiyo Yuden Co. Ltd	Japan	Electronic components	Flexible DSC using Ti foil as counter electrode for a sub module of 15×15 cm^2 (o.3 mm thin), test race car using 2×8 m^2 connected sub-modules in world solar car rally in 2008 and achieved a speed of 11.8 km/h in cloudy weather which was almost similar to 12.5 km/h in sunny weather.
15	SONY Technology Centre	Japan	Electrical appliances	Started research on DSC in 2001, applications for terrestrial power and indoor electronics, achieved 11.1 % confirmed η in 2009 (APL, 94(073308)), "Hana-akari"a solar lamp powered by DSCs developed.
16	Shimane Institute of Technology	Japan	Governmental organization	J2 dye, large area DSC (1.25m × 0.75 m) developments and stability testing for 1000 h at 80 ^oC, 'EneLEAF' in collaboration with Nissha. Ltd.
17	Toyota/ Aisen Seiki	Japan	Components and systems for automotive industry	One of the earlier industrial R&D on DSMs, S-type monolithic connections, stability test in outdoor exposure in 2006 for 2.5 years.
18	Peccell Technologies, Inc.	Japan	Venture company of Toin University of Yokohama	Plastic modules of DSCs, 4 V in a serially connected module of 10 × 10 cm^2, The world largest fully developed plastic modules (0.8 × 2.1 m) is the lightest DSMs weight (800g/m^2) with a capability of providing >1000 V.
19	Eneos Co. Ltd	Japan	Iol company but established a joint sub company named as 'Sanyo Eneos Solar Co. Ltd.'	Bi-layer photoanodes, solid state DSMs (10 ×10 cm^2).
20	NGK Spark Plug Co., Ltd.	Japan	Spark plugs	Started DSC research in 2003, adopted lithography in monolithic module fabrication, founder of ball grid DSC structures which replace Pt for catalysis purpose and utilizes 95% active area.
21	ITRI Taiwan (Industrial Tech. Research Inst. Of Taiwan)	Taiwan	Applied research and technical services	Transferred technology to Formosa Plastics and the mass production is expected at 2015.
22	Mitsubishi paper mills	Japan	Paper, pulp, and photosensitive materials	D-series dyes or indoline dyes perform better with ZnO due to metal free nature.
23	Panasonic Denko Co. Ltd.	Japan	Branch company of Panasonic, electronic appliances	See-through modules for indoor applications, stability testing and encapsulation to prevent electrolyte leaking, use of K9 dye instead N719 to improve stability.

24	KIST (Korean Ins. Of Sc. and Tech.)		Material for DSCs and device development	Flexible DSC especially stainless steel based devices with η ~4.2% higher than plastic based DSCs, molecular engineering helped in achieving an PCE of 11% at their labs, the technology is transferred to Dongjin Semichem Ltd.
25	J touch Taiwan	Taiwan	Touch panel solutions	Started indoor electronic by DSCs such as in portable time clocks.
26	Fraunhofer ISE	Germany	Environmentally friendly energy harvesting and storage research	Scalable development and stability research on DSMs, first large area (30 ×30 cm^2) glass frit based module design with thermal stability testing till 80 ^oC.
27	Institute of plasma Physics (CAS, China)	China	Utilization of the fusion energy	500 W DSC power station was installed in 2004 with η ~5.9% in parallel module, research is oriented on photoanode optimization, device packaging and interconnections.
28	ECN (energy research center of the Netherlands)	Netherlands	Energy research institute	First EU lab for DSC development started in 1995, stability tests for 1000 and 10,000 h, introduced master plate design, installed semi-automated DSC manufacturing up to 100 cm^2.
29	Gunze Ltd.	Japan	Electronic components and garments	Wearable DSC a unique application (28 cells with required electronics are attached to a jacket and used as mobile charge).
30	Yingkou OPV Tech New Energy Co., Ltd.	China	Up scaling DSCs/DSMs	Colorful, artistic and transparent DSMs in form of glass windows, and screens. Flexible and portable DSMs are also manufactured and available for commercial use.
31	Ricoh	Japan	Electronic (imaging and printing device, for example)	*s*-DSMs for indoor lighting.
32	Merck	Germany	Chemicals and pharmaceuticals	Electrolytes for DSCs, precursors for various photoanode materials.
33	Acrosol	Korea	Research & development, solar panel manufacturer	NA
34	NLAB Solar(name changed to exeger)	Sweden	Industrial production of DSMs	Pilot plant installed for the production of DSMs as BIPV and AIPV.
35	Dyetec Solar (Dyesol-Pilkington JV)	USA/Global	DSMs in BIPV	Joint venture of Dye-sol and Pilkington.
36	Tata Steel Europe	India	Steel roofing	Joint venture of Dye-sol and Tata Steel.

5. Current research on dye solar modules

Several major advancements have been made to upscale DSMs in terms of their various interconnection designs, material components, scalable fabrication processes, outdoor stability testing, tandem cells/modules to absorb wider light over solar spectrum, and innovative applications such as a hybrid energy harvesting and storage device. The advancements are paving the way towards the ultimate goal of the technology; their successful commercial deployment as a fossil fuel alternative and compete cost effectively

with the incumbent photovoltaics. Many developments are witnessed in the scalable production of DSMs such as fabrication of modules up to 8.2% certified η,[84] emergence of *s*-DSCs and *s*-DSMs to enhance the device lifetime,[85-87] initiation of flexible DSMs and their low temperature processing,[44, 46] long term stability and thermal testing of transparent conducting oxide (TCO) based DSCs up to 80 ^{o}C,[81,119] and their application as smart windows.[88, 89] The recent achievements such as the first commercial large scale delivery of DSMs from Solaronix, high efficiency *s*-DSMs from Dyesol (announced η ~11.3% at 1 sun, results are to be published yet),[90] and the thermal stability testing up to 90 ^{o}C further orient the successful commercial production of DSMs.[91] Figure 9 shows a timeline of DSMs development since the first report in 1996 till 2014. It highlights the major achievements of DSMs and also projects their potential future. In this section, we briefly review various developments in DSMs fabrications techniques and various designs.

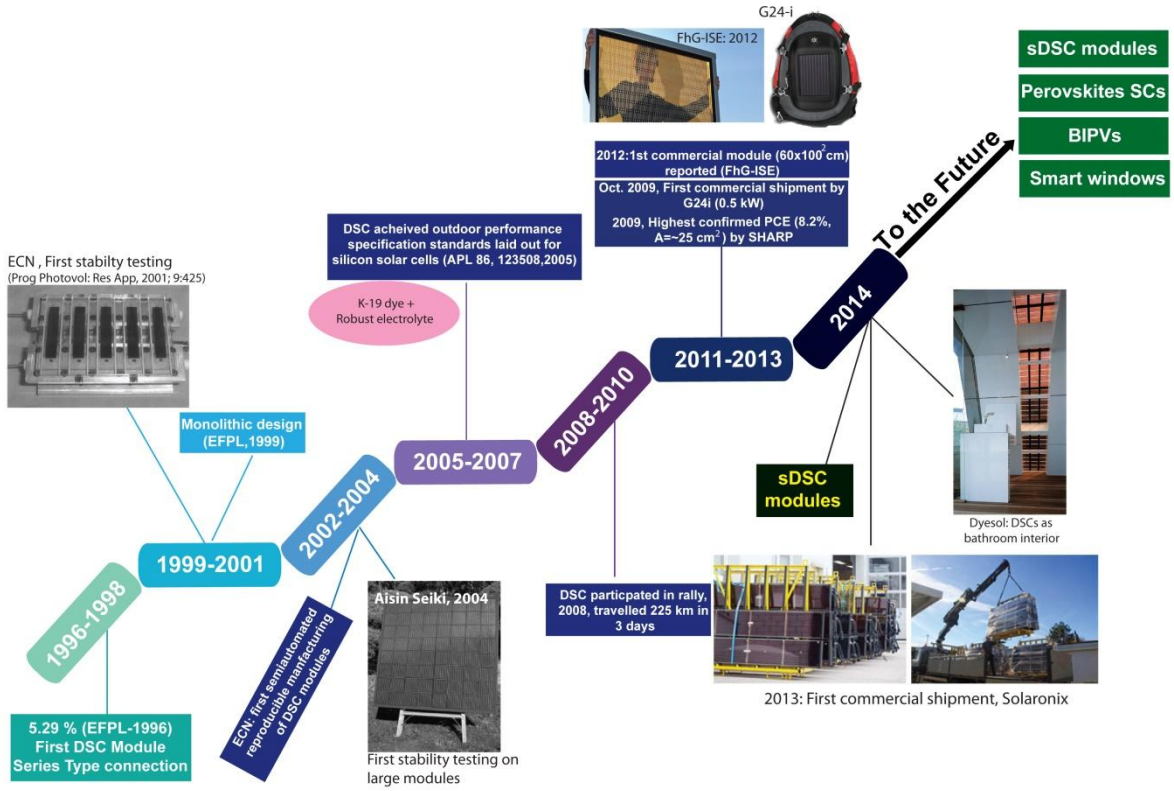

Figure 9: Step-by-step historical evaluation of dye-sensitized solar modules.

5.1 Fabrication processes of dye-solar modules

The fabrication of DSMs differs from that of single cells primarily due to the electrical connections among neighboring cells. Screen printing is usually employed as a coating method for photoanodes of DSMs,[92, 93] as it permits the facile and controlled deposition in the few to 20 μm thickness and is also compatible with roll-to-roll processing. Besides, the technique also offers compactness and good adhesion of TiO_2 with the substrates which otherwise often peels off from the surface upon annealing. Screen printing technology is a commercially available method for printing arts and can be used for printing on both glass and plastic substrates. Figure 10 shows a block diagram of various processes involved in DSMs fabrication. For details of each section, we refer to the pioneering work by Spath *et al*.[94] and a recent review by Hashmi *et al*.[57]

The working and pre-drilled counter electrodes are cleaned using trichloroethylene, acetone and ethanol. The electrodes are then etched for series connections. CEs are platinized by depositing Pt precursor pastes and then cured in a furnace.TiO_2 layers are coated on the working electrode (WE) via screen printing to get a desired photoanode thickness (~10 μm). A heat treatment (100 ^{o}C) after each coating cycle is helpful to obtain stability of each layer. In a batch process, the coated FTOs are heated on a belt furnace to remove organic binders in the paste and to sinter TiO_2 nanoparticles together. Interconnections (series) or current collecting fingers (parallel) between neighboring cells are made using conducting media (such as silver). The WEs are sensitized with a dye and device is completed by placing the patterned CEs on the WEs with 30-60 μm thick spacer between them and sealed. The Ag patterns are encapsulated to avoid their contact with the liquid electrolyte. Electrolyte is filled through drilled holes and after filling, the holes are sealed via cover slips and sealant material.

The typical dye-sensitization methods are not suitable for DSM batch production as it require longer soaking hours. Accelerated dye-sensitization process are introduced which require few minutes for dye-anchoring and yield similar photovoltaic performance to that of typical overnight soaking. Such accelerated methods may reduce the batch production time significantly. ECN researchers introduced a novel dye-anchoring method where they pumped the dye solution in a pre-sealed DSM through two drilled holes.[95] Such method is beneficial when the device is to be sealed using glass frit that requires high temperature (~500 ^{o}C) for adhesion; at which temperatures the dye decomposes. During DSMs fabrication, encapsulation and electrolyte filling are amongst crucial steps. Good encapsulation is crucial for long lifetimes and improper filling would lead to significant performance degradation for similar type of devices. At present, many of the researchers use pre-drilled holes at CE to inject the electrolyte via vacuum filling. This process is however tedious and a number of automated units for electrolyte filling are now offered by various companies such as Dyesol Ltd. easing the continuous production of DSMs.

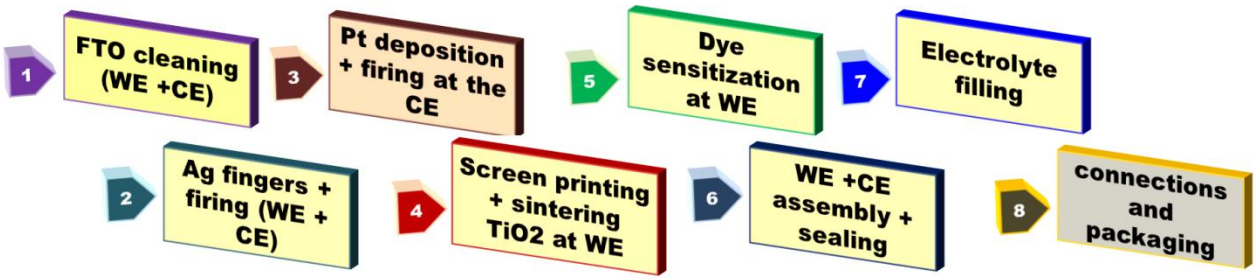

Figure 10: A schematic of a parallel DSMs assembly line. The figure is drawn based on the references[96, 97] which outlines the steps for parallel modules. For series connected modules the FTO has to be scribed for cell isolation. The W-type modules requires no Ag interconnections and for the Z architecture the order of the steps can change. For more detail on series modules fabrication, we refer to the reference 96 and 98.

5.2 Design configurations of dye solar modules

After intensive research for nearly two decades, commercial DSMs developments are underway (Table 2). The fabrication of DSMs is different from a laboratory scale device due to (i) large scale metal oxide coating on TCOs, (ii) extensively impermeable sealing to humidity, air and to prevent liquid electrolyte from drying and leaking, (iii) electrolyte filling, (iv) interconnection for modules (series or parallel) and external electrical connections, and (v) the most important is the anticipated lifetime of the device compared to that offered by silicon based devices (~20 years). Electrical connections need intensive care during fabrication process as an ineffective contact will ultimately lower FF by adding to the series resistance and eventually lowering the η.[98, 99] Two major types of connections are employed for DSMs fabrications, (i) parallel designs which provide high photocurrent such as parallel grid connections and (ii) series designs for high output voltage including Z-type, W-type, and monolithic connections. These designs employ large rectangular strips (area $\geq 3 cm^2$) interconnected serially or in parallel as shown in Figure 11(a-e). Other types of connections such as master plate design and ball-grid connection are reported by few researchers.[128,129]

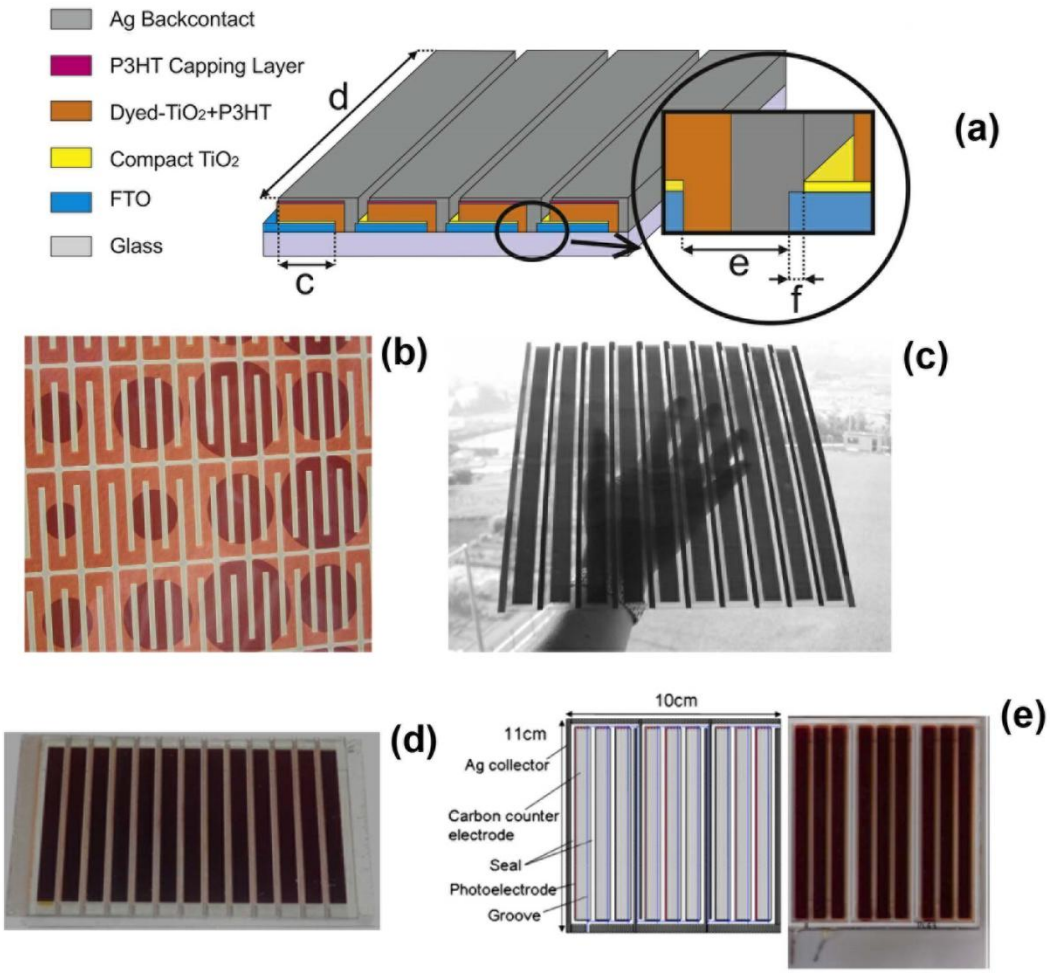

Figure 11: Some common adopted designs of conventional DSMs. (a) design schematics of sDSM employing P3HT (Poly(3-hexylthiophene-2,5-diyl)) as a hole transport media,[87](b) DSMs design for façade application under a Euorpean project COMSOL,[100](c) a flexible plastic DSMs,[101](d) a series Z-type module,[102] and (e) a parallel grid type design where the individual strips are surrounded by a metallic curent collector.[103] Other common architecture involves the W-type and monolithic designs for series connected DSMs (not shown).

In this section, we highlight the differences in these various interconnections, their advantages and disadvantages and also critically analyze their photovoltaic performance. For convenience, we define three common terms (active area, aperture area, and total area) that will be intensively used in this article. Active area is the area covered by only the TiO_2 strips on a substrate; aperture area is the sum of active area and the region between the cells (which are occupied by the sealants, interconnections or collecting grids); and total area is the total

substrate area which also includes the periphery area used for bus bars and blank spaces on the substrate.

5.2.1 Series connections

i. Monolithic design (S-type)

The term monolithic here refers to deposition of electrode material layers sequentially by pasting and pressing them successively. The monolithic DSMs are attractive as they are made on a single substrate (Figure 12a) and eliminate the need for the CE. Owing to their single substrate architecture, monolithic designs are highly compatible with roll-to-roll processing of flexible DSMs as they do not require continuous photoanode thickness.[104] The fact that the device is fabricated layer-by-layer, rather than by assemblind two electrodes together, make this design more tolerant to substrate non-planarity. These designs also replace expensive platinum by cheaper carbon black as CE; therefore, 20–30% of material cost reduction is estimated in monolithic type of series modules designs compared to the other designs.[105]

Monolithic design is also called Kay cell, named after the inventor Andreas Kay, who reported the first DSM in 1996 with η ~5.3%.[60] The notable achievements in their report are (i) replacement of expensive platinum with porous carbon as CE, (ii) a porous insulating layer between WE and CE to avoid short circuit but letting the electrolyte diffuse through its pores freely, and (iii) a continuous, conveyerized fabrication process of series connected DSMs. Thickness of the photoanode in Kay cell was ~80 µm (TiO_2 10 µm, Rutile spacer 10 µm, & carbon black 60 µm). The DSMs (six strips of 4.7 × 0.7 cm^2 and total area ~21 cm^2) yielded η ~5.3% (V_{OC} ~3.90 V, I_{SC} ~28.55 mA, & FF ~0.61). Major drawbacks of this design are much lower J_{SC} (1.3 mA/cm^2) despite a high output voltage ~4 V, high opacity, and poor

sealing of the device. ZrO_2 is also employed to replace opaque rutile spacer; however, the transparency was lower than that of a conventional Pt electrode.[104]

Since the first report on series interconnections, there has been no significant progress in these designs. Thirteen years after the work of Kay in 1996, improved transparency of the monolithic designs was reported by AISIN SEIKI.[106] They replaced (i) the opaque counter CE material (carbon black) by a highly transparent paste comprising In_2O_3:Sn and Pt nanoparticles and (ii) opaque rutile spacer by SiO_2 (refractive index 1.5, close to that of electrolyte used) thereby improving the transparency considerably. The photovoltic performance of their module was rather inferior than the first report; the four times larger modules developed by AISIN SEIKI (95 mm × 95mm, area ~91 cm^2) resulted in 30% incereased J_{SC} (~1.7 mA/cm^2) compared to the Kay's first design (area ~21 cm^2). The lower J_{SC} limited the η to be <3% despite a higher output voltage (~8 V).

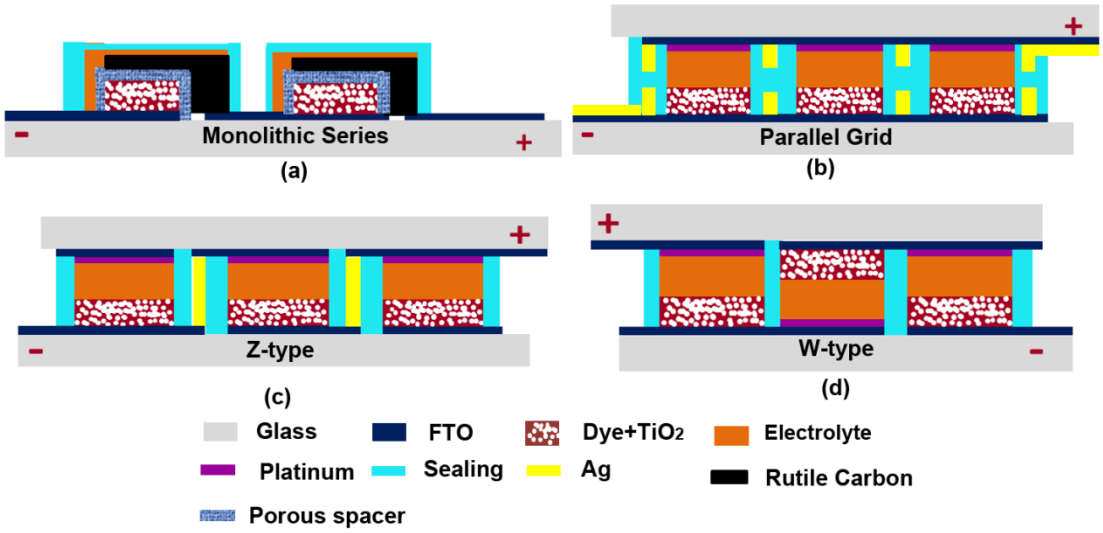

Figure 12: Schematic of series type of connections (a) monolithic, (b) Parallel grid (c) Z-type and (d) W-type.

Monolithic DSMs are built on a single subtrate (WE only) and therefore known as a cost effective design. Another major advantage of this design is the high active to total area ratio. In both reports on monolithic designs, this ratio was >90%. However, these connections

result in lower J_{SC} due to high series resistance and low FF ($\leq$ 0.6) thereby.[106, 107] As the individual strips are connected in series, immense attention is to be given to match the J_{SC} in all individual cells. Due to series type of connection, the final J_{SC} will be the lowest one in the serially conencted cells. Monolithic transparent DSMs on a single substrate with high transprency are yet to be seen.

ii. Z-type and W-type interconnections

Both these types are series connected devices: one of them uses a vertical metallic conductor to connect the neighbouring cells (Z – type) whereas the other (W – type) does not require it (Figure 12 c& d). The names 'Z-type' and 'W-type' stem from their resemblance to 'Z' and 'W' alphabets, respectively. The Z-type connection, also called Z-contact, is adopted from thin film solar cells.[104] In this design the individual cells are serially interconnected via a conducting medium (usually silver) in a way that the CE of the first cell is connected to the WE of neghbouring cell and vice versa as shown in Figure 12c.

The first Z-type DSM was demonstrated in 2004 by Toyoda *et al*.[108] who connected 64 DSMs (10 × 10 cm^2) in series to form a large panel. The researchers carried out the first long term stability testing of DSMs for six months and compared the performance with a crystalline silicon module of similar output power rating. Although photovoltaic parameters of DSMs are not exlusively reported the DSMs showed 10 – 20% larger power output for a period of six months. The major issue reported during fabrication is the hermetic sealing of the DSMs which resulted in performance degradation. This issue is resolved in a subsequent report by Sastrawan *et al*.[95] who introduced a highly stable glass frit as a sealent. As the frit is to processed at high temperature (>500 ^oC), at which temperatures the dye decomposes, a novel pumping method for dye anchoring was employed. The dye was pumped via two holes after the sealing of DSMs of total area upto 30 × 30 cm^2. The DSMs resulted in η ~3.5% (V_{OC}

~20 V, I_{SC} ~168 mA, & FF ~0.53) with an active area ~680 cm^2 (74% of total area). The major drawbacks of these reports are the low FF (<0.55) and low J_{SC} (<0.5 mA/cm^2) arising from the high series resistance of photoelectrodes. Jun *et al.*[107] reported a DSM (10 × 10 cm^2) resulting in sigificantly superior performance, i.e., η ~6.6% (V_{OC} ~8V, J_{SC} ~1.23 mA/cm^2, & FF ~0.67). The significant enhancement in FF and J_{SC} is achieved by restriciting the width of each individual strip (<1 cm). A similar advancement is reported by Giordano *et al.*[102] by optimizing the geometry of the photoelectrode and using a back reflector to achieve η up to ~7% on apaerture area in modules of ~45 cm^2 area.

Despite the high acheiveable voltage by Z-type DSMs, it can suffer from relatively low active area due to the vertical connections and surrounding sealings, complexity of fabrication and the additional series resistance offered by added interconnection which can reduce the fill factors. Furthermore, the silver interconnects corrodes easily in the presence of liquid electrolytes. In an innovative design by Dyesol, the silver is repalced by less corrosive material (titanium particle of size 45 μm and tungsten particles of size 5 μm in a polymer matix).[109]Although presumambly the vertical connections are less conductive, per unit section, than Ag, besides adding stability to the device, this design also eliminated some additional sealing to protect the interconnections required by the Z-type.

The W-type design offers comparitivly higher active area than Z-type as it avoids additional metallic interconnections.[104]Unlike the Z-type, the neighbouring cells of alternative bias are interconnected in W-type as shown in Figure 12(d). Their simpler design and no additional serial interconnections can result in higher FF in the devices. The operation of W-type DSMs is different from Z-type as on the same module there are two types of cell configurations, i.e., front illuminated (TiO_2 side, also called F-side) and back illuminated (Pt side, also called R-side). The issue with W-type designs is the difficulty to match the J_{SC} in these two different types.[98] The J_{SC} decreases in the R-side due to light absorption by

iodide/triiodide and low transmittance of platinum.[84] Thus, many optimization procedures to match the J_{SC} of both types add complexity to fabrication. Yet, SHARP Co. reported the highet confirmed η in W-type interconnected DSMs (8.2% and 9.3% with respect to active and total area, respectively). The active area (25.45 cm^2) was 85% of the total area.

One crucial requirement for both Z- and W-type designs is the seperation required between neighbouring cells to avoid mass transfer of electrolyte.[104] As the redox potential of the electrolyte changes when illuminated, a possible ion exchange between adjacent cells would separate the redox couple. This process is called photophoresis and is responsible for performance deterioration over time in DSMs. Thus an individual cell has to be a completely isolated compartment.

5.2.2. Parallel connection

Despite high V_{OC} by series interconnected DSMs, the required precision to match the J_{SC} of individual cells and intensive care to interconnect the neighbouring cells to avoid lower FF and metal corrosion make their design and fabrication complex. On the other hand, parallel grid type DSMs offer ease of fabrication as they avoid interconnection of working and counter electrodes (Figure 12b). An example of such connections is the 'masterplate' designed by a joint research of various European institutions under the programme Nanomax.[128] In parallel connections, charge is collected not only from the bottom of the electrode in contact with the FTO but from the sides of the strips also by using a metal grids (Ag, Ni, Cu Al, and Au).[49,110-114] These metals grids significantly enhance the photovoltaic performance of DSMs; 100% increments in J_{SC}, >200% increment in FF and 5 folds enhancement in η is reported when silver grids are coated around large strips.[144] Spath *et al.*[125] reported a reproducible manufacturing of parallel connected DSMs (27 DSMs with total

area ~100 cm^2) with η ~4.3±0.07%. This method is further developed to deliver η ~7.4% employing silver as current collecting grids.[115]

These designs can result in high FF but the major drawback is the low active area due to silver current collectors which need to wide enough to collect the high currents with minimal voltage drops. Care must also be put in avoiding corrosion of silver grids by the iodide/triiodide electrolyte, for example,by using thick spacers (Surlyn or Bynel) covering the grids.[57, 104]

5.2.3. Ball grid DSC (BD-DSCs)

Ball grid connection (based on ball grid array connection in electronic circuits) was introduced by NGK Spark Plug Co., Ltd., Japan to overcome lower FF when the electrode width was increased beyond a critical size.[43, 116] This critical width is determined to be ~0. 5 – 1 cm^2 such that the ohmic resistance of the film is reduced and offers higher FF.[102, 117] The ball grid design (Figure 13 b&c) resembles monolithic designs as it employs only one substrate (FTO). These modules are connected in parallel and employ vertical metallic balls as current collectors; the major difference is that the electrons and holes are collected at the same side unlike all other designs where electrons are collected from the FTO (Figure 13c). The vertically oriented balls are then connected to a flexible hybrid copper polyimide substrate and are taken to the external circuit. Surprisingly, the DSMs of 8 × 8 cm^2 area resulted in similar performance to that of a single cell (area ~0.5 cm^2); the DSMs showed η ~7 – 8% (J_{SC} ~16 mA/cm^2, V_{OC} ~760 mV, FF ~0.65) with V_{OC} higher than that of a single cell. The remarkable performance of ball grid, which can also bring commercial advantages, is due to their ability to retain the performance of a single cell during scale up process and also due to their cost effectiveness as they eliminate the expensive Pt coated CE. These

designs do not require additional interconnections and external electrical connection; and therefore, result in very high active area (95%) as shown in Figure 13(b).

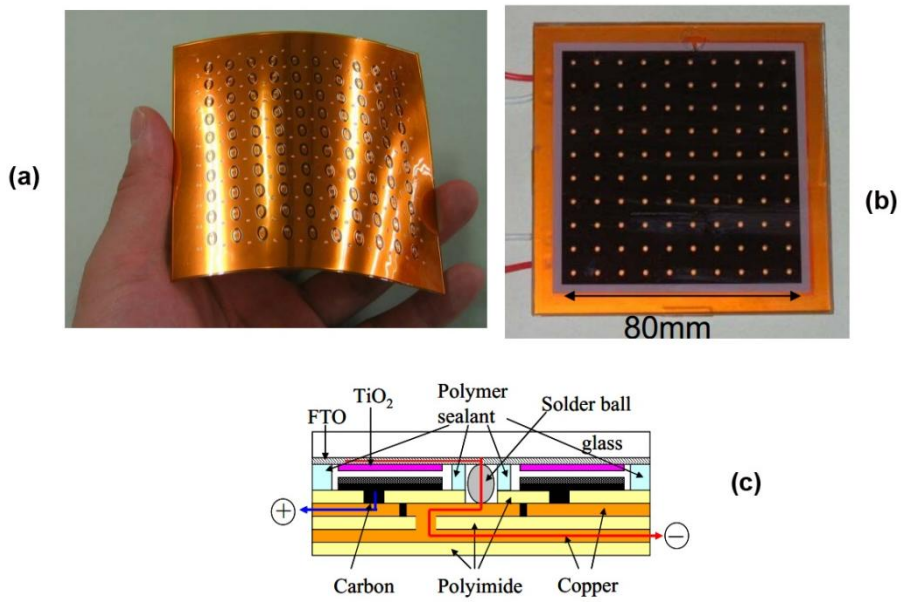

Figure 13: (a) solder shape ball connects on flexible copper polymide substrate, (b) an 80 mm square sub-module with η 7-8%, and (c) cross-section of a ball grid DSM. Figures are taken from an online report from NGK Spark Plug.

5.2.4. Combined Series and Parallel connected DSMs

Until now we have discussed various series or parallel connected DSMs which provide either added photovoltage or photocurrent, respectively. In such designs, one of the two parameters is compromised; the DSMs with high V_{OC} result in very low J_{SC} and vice versa (Table 3). To control the value of both of these parameters in a single device, which may be important for managing the electrical output of the module, a combination of series and parallel connection is also attempted by researchers (Table 3).[148,149] Such dually interconnected best performing device so far resulted in η ~6% (V_{OC} ~1.4 V, I_{SC} ~ 287 mA , FF ~0.56) in a device of area ~90 cm^2. The issue here is very low active area; ~50% of the total area is utilized for additional interconnections. Nevertheless, such designs are desired, especially, while designing large area panels as will be discussed in section 8.

6. Fabrication of flexible modules

At present, the automated manufacturing of DSMs has steps (Figure 10) that still require development for a high volume low-cost production. The rigid glass substrate used for DSMs manufacturing and the high temperature required to evaporate the organic binders in the TiO_2 paste and electrolyte insertion are typical issues in the batch production of DSMs. Alternatively, various flexible substrates are introduced which are compatible with roll-to-roll process.[118-121] Besides flexibility, these substrates are also cost effective. For example, commercial plastic substrates (PET/ITO) available from Solaronix cost only one third to that of FTO coated TCO.[122] Note however, that additional encapsulation may be required, especially for long term outdoor operation, which can offset these cost lowering. However flexible devices are very desirable for applications where light weight, conformability, flexible, thin power sources are sought. Furthermore roll-to-roll high-throughput manufacturing can be applied.[19]

To utilize the flexibility of these substrates, various researchers replaced the conventional FTO coated TCOs with conducting plastic[123] and metallic substrates such as Ti foil or steel (Table 3).[124, 125] For developmental history of flexible DSCs and DSMs (*f*-DSMs), we recommend the comprehensive review by Weerasinghe *et al*.[126] and also by and also by T.M. brown *et al.*[19] The first report on *f*-DSMs utilized a stainless steel substrate as WE and Pt coated flexible plastic as CE and demonstrated η ~3% (V_{OC} ~6.5 V , I_{SC} ~47 mA, FF ~0.33).[124] The observed low FF in less resistive metallic substrate is surprising, which was attributed to high series resistance. However, a reference single cell also showed similar FF and J_{SC} (~8 mA/cm^2); therefore, the low FF could be due to poor device fabrication and poor contact between the substrate and photoanode layer. Such poor performance of a metallic

substrate is later improved by employing a Ti foil and growing vertically aligned nanotubes of ~35 μm by Jen *et al*.[123] They employed a Pt coated flexible polyethylene naphthalate (PEN)/ITO as CE. A parallel connected *f*-DSM (~5.5 cm^2) resulted in η ~4.8% (V_{OC} ~ 0.76 V, J_{SC} ~13 mA/cm^2, FF ~0.54). Here, a better contact between TiO_2 nanotubes and Ti foil resulted in significantly improved performance; however, stability of the devices is not addressed so far. Conducting plastic substrates (PET/ITO and ITO/ PEN) are widely employed as substrates in *f*-DSMs owing to their transparency. Ikegami *et al*.[101] reported η ~2% (V_{OC} ~6.6 V, I_{SC} ~77 mA, FF < 0.50) in DSMs (30 × 30 cm^2) on a PEN substrate. The corrosive electrolyte badly affected the performance of these *f*-DSMs over time; the performance degraded ~40% after ~1000 h primarily due to removal of ITO from the substrate caused by the reaction with electrolyte.

A mass production compatible process for the TiO_2 paste application is an elusive issue. Various methods employed so far such as anodization,[127-129] lift up technique for a mesoporous highly conductive TiO_2 layer,[130] compression method to enhance TiO_2 film interconnection,[131-135] and printing of binder free paste via doctor blading,[118, 136] hinders the roll–to–roll production of *f*-DSMs. Zardetto *et al*.[46] employed a UV irradiation process for fabrication of both working and counter electrodes which is compatible with roll–to–roll process and showed (i) η ~4.3% (V_{OC} ~0.73 V, J_{SC} ~11 mA/cm^2, FF ~0.56) in single cells and (ii) η ~3.3% (V_{OC} ~3.8 V , J_{SC} ~1.8 mA/cm^2, FF ~0.53) in W-contact modules of area ~17 cm^2. In another comparative study on the performance of flat and bent *f*-DSM, the same group showed that DSMs when bent can yield 10% extra power output compared to a flat device.[44]

The flexible DSMs routinely demonstrate lower FF and J_{SC} resulting from high sheet resistance due to the poor contact of the mesoporous layer with the substrate and higher sheet resistance of the conducting substrates.. Addition of thin TiO_2 layer via $TiCl_4$ solution

treatment is a common practice in conventional DSCs to improve adhesion of photoanode layers.[137-139] However, it cannot be applied on *f*-DSMs as it requires annealing at 450 ^{o}C before coating mesoporous TiO_2 layer. The flexible plastic substrates are not compatible with such high temperature. Replacing conducting plastic with low resistive metallic substrate such as steel did not show a significant progress. Ti foil, however, is an often used material in this regard as TiO_2 nanostrucutres can be grown directly onto it and there are no adhesion issues between the substrate and the mesoporous layer. A report by Wu *et al.*[140] made a significant development towards this end and reported η ~7% (V_{OC} ~0.72 V, I_{SC} ~727 mA, FF ~0.73) at 55 mW/cm^2 in a flower shaped mesoporous film directly grown on Ti foil. High FF and J_{SC} (~8 mA/cm^2) are achieved due to the absence of additional interconnections thereby resulting high ratio of active to total area of the device (>90%) . However, the η reported is at 55 W/m^2; therefore, a correlation of the performance of *f*-DSMs with the high efficiency DSMs on TCOs is not straightforward.

7. Emergence of solid state DSMs

Although the *l*-DSCs have achieved η>8% in DSMs and ~13% in DSCs, they are susceptible to performance degradation due to leakage and the change in redox species concentration during regeneration process.[81,] Furthermore, electrolyte insertion is not a trivial process over large areas. Because of these issues DSMs with alternative HTMs such as quasi-solid state electrolytes[141] and solid state hole conductors are tested.[85] The *s*-DSMs using HTMs are relatively new and only few reports are published. The first report on *s*-DSMs employed poly-methyl-meta-acrylate (PMMA) and propylene carbonate to make a gel of the conventional iodide/triiodide electrolyte.[141] Their series connected DSMs of 100 cm^2 resulted in η ~0.8% (V_{OC} ~ 5.16 V, I_{SC} ~37 mA, FF ~0.47). They also demonstrated that *s*-DSMs can be fabricated without sealing the neighboring cells; however, the performance of such DSMs

dropped 60% in ~1000 h. Their up scaled *s*-DSMs of size up to ~625 cm^2 (23 serially connected DSCs of active area ~12.5 cm^2) showed relatively inferior performance than that of DSMs of total area ~100 cm^2; the η dropped to 0.32% mainly due to decrease in I_{SC} (28 mA) and FF (0.35). The lower FF and J_{SC} (2 – 3 mA/cm^2) in both DSMs is primarily due to high series resistance (200 – 400 Ω) and reduced TiO_2 thickness (4 – 4.5 μm) compared to a conventional photoelectrode (15μm), respectively. On the other hand, these modules showed slight improvement in performance after 1000 h unlike the liquid based DSMs (*l*-DSMs). In a similar report, Freitas *et al.*[142] employed plasticized polymer electrolyte based series connected *s*-DSMs (4.5 cm^2). Although a high V_{OC} ~8V is obtained in outdoor testing, the low I_{SC} (~ 20mA) resulted in a lower η < 1%. Furthermore, the performance of these *s*-DSMs is rather discouraging after 1800 h and the devices retained only 30 – 40% of original power output.

Unlike the *l*-DSMs, the performance of *s*-DSMs is significantly inferior to their single cells. In a comparative study by Snaith *et al.*[86] serially connected 8 cm^2 *s*-DSMs employing mesoporous TiO_2/Al_2O_3 and spiro-OMeTAD showed η ~2% (V_{OC} ~1.5 V , I_{SC} ~35 mA, FF ~0.47), merely 25% of a reference single cell of area ~0.12 cm^2. Low pore-filling (~40%) is found to be one of the factors contributing to low η in their modules which can be improved by changing solvent concentration of HTM and porosity of the photoanode film. In a similar report by Matteocci *et al.*[87] η ~2% (V_{OC} ~0.3.2 V , I_{SC} ~22 mA, FF ~0.39) on a TCO based device is reported on an active area of ~14 cm^2. The η is ~6.7% in flexible *s*-DSMs fabricated on Ti foil.[140] The researchers employed P3HT as HTM with TiO_2 nanoparticles photoanode.

The performance of *s*-DSMs is mainly hindered due to the poor infiltration of HTM into mesoporous photoanode unlike the liquid electrolyte which easily penetrates throughout the TiO_2 film (~15 μm). Owing to the inferior pore filling (~40% in both the reports where *s*-

DSMS showed η >2%), the TiO_2 photoanode thickness is restricted to ~2 μm and thereby yielding only 30% of J_{SC} to that of a *l*-DSMs. The pore filling could be improved by using tubular or hollow nanostructures with high porosity (>60%) instead of nanoparticles enabling thus to increase the layer thickness ≥10 μm. If these issues can be resolved, together with developing semi-transparency (i.e. for BIPV) for thus type of devices, the future of *s*-DSMs has strong industrial potential since they do not use volatile liquids, an issue for lifetimes, and fabrication costs of *s*-DSMs is expected to be cheaper than *l*-DSMs as they require less complicated sealing during fabrication.

8. Dye solar panels (DSPs)

For realistic commercial applications, DSMshave to be transformed into larger panels for installation. The primary difference DSMs and DSPs is their size, even though there is no clear description of size limit. In this article, we define a panel when photoelectrode size ≥1000 cm^2.

Numerous industrial developments can be seen across the globe for the DSPs (Table 2); however, only few experimental results are published on their performance.[100, 143] The first panel was reported in 2008 with a total area >2 m^2, the invidual modules were of area ~300 cm^2 each.[113] The dually interconnected panel resulted in η ~6% on active area (V_{OC} ~9V, I_{SC} ~2.1 A, FF ~0.62) at 0.87 sun. This η is the highest reported for DSPs so far. Subsequently a joint Euorpean project termed 'ColorSol' was established to develop DSPs for BIPV applications.[100] DSPs of area upto ~14000 cm^2 (serially connected individual modules of area ~900 cm^2) resulted in η ~3.6% (V_{OC} ~4.55 V, I_{SC} ~945 mA, FF ~0.56) with respect to total area under 1 sun conditions (η = 4.6% with respect to its active area) was developed under this program. These panels employed glass frit as sealing material; and

therefore, reported high stability (~500 h). Both these panels were manufactured by serially inerconnecting individual DSMs; and therefore, the main issue in upscaling the DSC technology, i.e., development of an automated process for large scale panel, still remains a challenge. A research by Hinsch *et al*.[143] reported a semi-automatic process for the fabrication of DSPs up to ~1 m^2, which is an industrially viable size. Although the performance of these panels were comparitivly low (η <3%) than previous reports this is the first published report on development of a semi-automatic reproducible process.

9. Summary of DSMs development

All these designs have relative merits and drawbacks. Monolithic series are good in terms of continuous industrial mass production and are cost effective however they compromise on performance because of pore filling issues. Similarly, parallel (Ag grid encapsulated) designs are being developed by companies such as 3G solar but they lead to problems for large areas as currents become so high as to cause problems in voltage drops. W-type is the simplest to makes but has problems with current matching which can limit efficiencies and stability. Z-type delivers good performance, although their manufacturing is more complex due to the vertical interconnections and their encapsulation.

Table 3: A comparison of PV performance and devices designs of a few DSMs is listed. The percentage of active to total area is also given for a meaningful comparison.

Connection type	Active Area (cm^2)	Active to total area	I_{SC} (mA)	V_{OC} (V)	FF	η (%)	Comments	Reference
Parallel (grid coated)	68	68%	NA	0.7	0.65	4.3	These designs are mostly grid coated using Ag or other metals such as Ni. This type of connection results in enhanced current density but creates stability issues in device. To avoid metallic grid exposure to electrolyte, it should be encapsulated into sealant thus adding complexity to fabrication process. The advantage of these designs is a more simple power management at the individual DSM level compared to series design where high levels of current matching are required. These designs also survive reverse bias degradation.	94
	187	62.3%	1296	0.7	0.52	4.84		110
	81	81%	820	0.7	NA	4.3		111
	75	NA	50	0.76	0.7	5.7		49
	2246	63%	2100	9	0.62	5.9[a]		113
	18	73%	235	0.63	0.67	5.47[b]		114
	151	67%	2287	0.72	0.68	7.4[c]		115
	15.12	60.5%	172	0.75	0.66	5.52		97
	17.11 (ap. area)	NA	19.4	0.719	0.71	9.9[d]		
Series+ Parallel	110	NA	120	2.2	NA	NA	This design reduces active area available on photoelectrode and provides lower J_{SC} but multiplies V_{OC}. The design is not widely adopted and has minimal scope for commercialization.	103
	NA	NA	23.45	1.85	0.58	3.[e]		144
	90	50	287	1.4	0.56	5.9		145
Z-type	43	73	51	9	0.65	7	Z-type DSMs provide good performance and high active area. However they can suffer from lower FF due to excess interconnections which adds to series resistance. Careful encapsulation of vertical connections is	102
	47.5	47%	58	7.7	0.68	6.6		107
	505	74%	169	20	0.53	3.5		146

	512	73%	140	29	0.58	4.5	necessary.	147
W-type	25.5	85%	54	6.3	0.61	8.2[f]	The highest certified efficiency reported in any DSM. However care design for current matching is required.	84
Series Monolithic	19.75	94%	28.55	3.9	0.61	5.29	Any mismatch of current in cells will affect efficiency of the module. This design yields lower current density.	60
	90.25	90.25%	40	9	~0.6	<2.5		106
Ball Grid	80	95%	~1200	0.76	NA	~8%	Very high active area, similar performance of that of a single cell.	116
DSCs (Single cells)	~0.2		4.6	0.91	0.78	13	Routinely reported J_{SC} values in best performing *l*-DSCs.	26
	0.2	--	~4.6	0.93	0.74	12.3		148
	0.22	--	4.57	0.73	0.72	11.1		149
***s*-DSMs/quasi *s*-DSMs**	100	~45%	37	5.16	0.47	0.8	Pore-filling, lower photoelectrode thickness, high stability	141
	625	46%	28	10.6	0.35	0.32		141
	112	52%	20	8	NA	0.9		142
	2.25	NA	20	0.62	0.50	2.8		150
	8	NA	~35	1.5	0.47	~2.5		86
	13.5	54%	21.5	3.2	0.39	2		87
s-DSCs	0.2	--	19.2	0.73	0.73	10.2[g]	The highest efficiency solid state laboratory scale device.	151
	58	~60-70%	47	6.5	0.33	~3		124
	900	NA	77	6.7	<0.5	2-3%		101

Flexible DSMs	5.4	NA	69[h]	0.76	0.54	4.8	Devices fabricated on conducting plastic (PET/ITO) or metallic substrates such as Titanium foil.	123
	16.4	69%	30	3.8	0.53	3.3		46
	100	90%	727	0.72	0.73	6.7[i]		140
Large area panels	2246	63%	2100	9	0.62	5.9[a]	As per the definition of DSPs in section 5.3, large area panels are ≥ 1000 cm^2.	113
	14000	74%	945[j]	4.5	0.56	3.58		100, 143
	6000	48%	--	--	--	2.3		143

[a] At 0.84 sun, 64 series and parallel connected DSMs;
[b] η 7% at 0.5 sun;
[c] CE consist of mixed Ti:Pt;
[d] The values is taken from reference 28, the original report stating the value is not found out in our search.
[e] 3D wire shaped DSM tree, I-V measured at 0.87 sun;
[f] the highest certified η in DSMs;
[g] reported η is without a mask;
[h] calculated with respect to active area only;
[i] Ti Foil as a substrate and photovoltaic performance is reported at 55 mW/cm^2;
[j] the reported photocurrent is only for a single DSM of area ~700 cm^2.

10. Emergence of alternative designs

10.1. Dye solar module designs with improve FF

As described in Table 3, various designs of DSMs, *s*-DSMs, *f*-DSMs and DSPs are fabricated to bring the device from laboratory scale to a level compatible with industrial mass production. These various types of connections resulted in devices with a voltage as high as ~20 V and a current as high as ~2.5 A in separate devices. However, since the first report on large area DSCs till date, lower J_{SC} is routinely observed in DSMs as compared to their single cells (Table 3). The highest confirmed J_{SC} in any DSM is ~18 mA/cm^2 reported by L. Han *et al.*[84] in W-type designs and by Giordano *et al.*[102] in Z-type designs but the routinely achieved J_{SC} is much lower than it. The highest J_{SC} in any other design is ~15 mA/cm^2 (in parallel designs). On contrary, the highest J_{SC} in a laboratory scale single cells is ~27 mA/cm^2,[35] and J_{SC} > 20 mA/cm^2 is commonly obtained in high efficiency devices as shown in Table 3.

This loss of 30 – 50% of generated photoelectrons in large area devices is crucial and seldom explained in the published reports. A few reports published on DSMs suggest that the comparatively lower J_{SC} in DSMs is due to increased series resistance (R_S) which also affect the FF of these devices. This increased R_S is originated from two sources (i) the width of the TiO_2 photoanode and (ii) the added metallic interconnections particularly in series type DSMs.[100, 117] The realization that TiO_2 width contributes to the R_S was first experimentally demonstrated in 2006 by Biancardo *et al.*[141] The researchers varied the TiO_2 strip thickness from 2 – 0.5 cm and suggested that the lower thickness results in superior performance of DSMs; however, a clear trend between FF and R_S could not be drawn from their experimental results. In a subsequent report, Jun *et al.*[107] demonstrated the effect of photoelectrode dimensions (length and width of TiO_2) and their effect on FF. They first optimized the TiO_2 strip width (W_S) to be 0.8 cm for optimum FF (~0.65 – 0.62) by varying it from 0.25 to 3 cm. The FF dropped drastically from 0.65 to 0.3 when W_S increased from 0.8 cm to 3 cm. On the

other hand, when the length (L) is varied from 5 – 15 cm by keeping the W_S ~0.8 cm, the FF showed no dependence on L. Similar dimensions are recommended by Zhang *et al.*[117] using simulation and by Giordano *et al.* [98] through experiments aimed to design guidelines for DSMs geometric parameters. The latter suggested W_S to be kept between 0.5 – 0.7 cm for photoelectrode length up to 15 cm as it provides a best compromise between aperture area and resistive loss. In another report, Giordano *et al.*[102] via modeling of geometric dimension showed a systematic decrease in FF is upon increasing the W_S from 0.5 – 2 cm. No effect is found on V_{OC} or J_{SC} of the devices upon varying the L. They correlated the R_{TCO} with photoelectrode dimensions (W_S, L, and distance to the collecting electrode 'd') as

$$R_{TCO} = R_{SHEET} \times \left(\frac{W_S+d}{L}\right) \quad (1)$$

Nevertheless, the optimization suggested in all these reports only involves minimizing the W_S to reduce the R_S offered by substrate. An increase in W_S is suggested as the primary source of elevation in R_S and thereby a drop in FF in all the above reports. However, even after minimizing the width of the individual strips to <1 cm, the performance of DSMs is only < 50 – 60% of that of DSCs at 1 sun.[152] The suggested optimization in these designs although improving the FF of the DSMs, added a number of interconnections reducing the aperture ratio of the modules. However, none of the reports on the optimization of device geometry discussed the reasons behind the low J_{SC} in DSMs. Furthermore, a comparative charge transport analysis of large area photoelectrodes with that of a single cell was lacking; and therefore, a detailed understanding of charge dynamic was surprisingly still missing in DSM literature.

10.2. Area dependent charge collection in DSMs

We note that all the adopted designs in DSMs are similar. In a common practice, these modules are made in the form of large rectangular strips (Figure 11 a–c) of an area ≥3 cm^2 interconnected in either series, parallel or both. Many of these designs are adopted from other PV technologies; the parallel or grid connections are adopted from amorphous silicon solar cells while the series interconnections are inspired from thin film modules. Recent studies by Fakharuddin *et al.*[153-157] suggest that these designs do not fit well for DSMs due to their diffusive charge transport in a "soft" environment which is largely different from the first two generation solar cells. It is noticed that due to negligence of charge transport parameters while up scaling the DSCs, significant current collection is only from a limited region of the photoelectrode. For example, at similar experimental conditions, ECN researchers obtained η ~12 % in their single cells and η ~4-5% in modules of ~225 cm^2 in a master plate design.[105] Such trends are routinely seen in DSMs; their J_{SC} (Table 3) values are significantly smaller than that of DSCs.

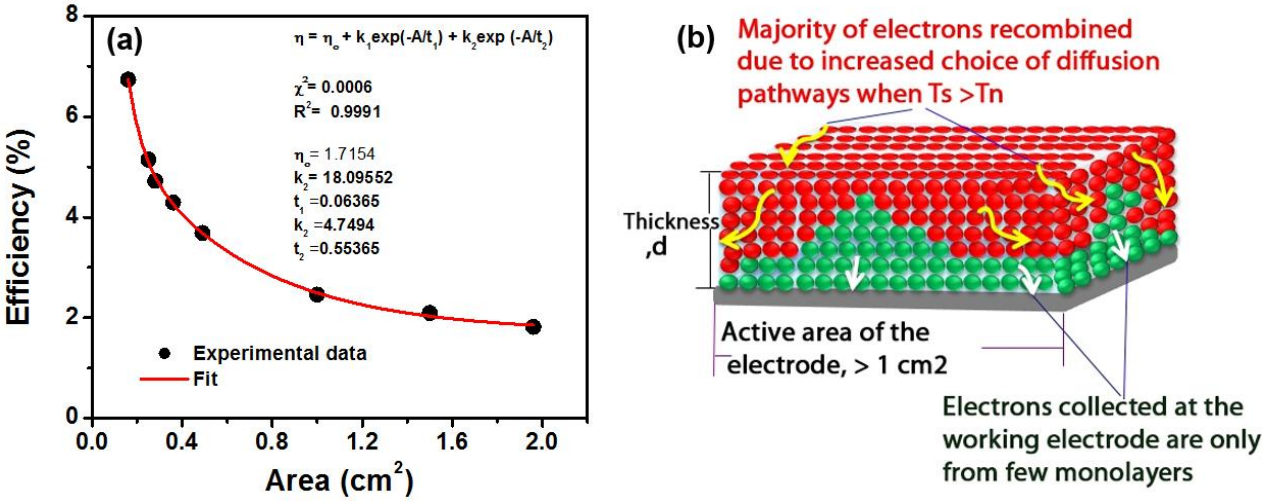

Figure 14: (a) The efficiency of a DSC decreases biexponentially with the increasing device area in a range of 0.15 cm^2 – 2cm^2, (b) schematic shows electron collection from only a fraction of the photoelectrode film nearer to the WE in DSCs of large photoelectrode area. Figure reproduced from reference.[154]

Important to note that the charge transport in DSCs is via hopping or trap-mediated conduction through n-MOS which is several orders slower than that through single crystalline semiconductors.[158-163] Due to diffusive charge transport and in a competitive situation where the generated electrons are rapidly intercepted by the ions in electrolyte, the photoelectrode thickness is limited below ~15 μm in single cells (area ≤ 0.2 cm^2). Currently, diffusion length ($L_n = (D_n.\tau_n)^{1/2}$) is the only defined parameter considered for complete collection of photogenerated electrons in TiO_2 film,[164-166] where D_n is the electron diffusion coefficient and τ_n is the electron lifetime. i.e., the length above which electrons recombine with holes in the electrolyte. In recent experiments it is noticed that the number of paths and path lengths of electron diffusion increases during scaling up; and therefore, the L_n as a device parameter has limitations in DSMs.[156, 157] We first reported that the η drops biexponentially upon increasing the active area in photoelectrode for TiO_2 NPs.[154] The η drops off 3 fold when the photoelectrode area is increased in the range 0.15 – 2cm^2; the main contributor to which is the drop in J_{SC} (Figure 14a). The detailed charge transport studies of these devices suggests that upon increasing the photoelectrode area, the recombination resistance (R_{CT}) decreases and electron transport time (τ_d) increases and consequently, photoelectrons from a fraction of TiO_2 (few microns) nearer to the working electrode are only collected as shown in Figure 14 (b). A similar idea is reported by Halme *et al.*[22] who suggested via device simulations that the possibility of electrons to be collected is higher if they are produced nearer to the working electrode substrate. As the τ_n is several tens millisecond in DSCs employing TiO_2 NPs, a high R_{CT} and low τ_d (10 – 100 times smaller than τ_n) is preferred for high efficiency devices.[20, 167]

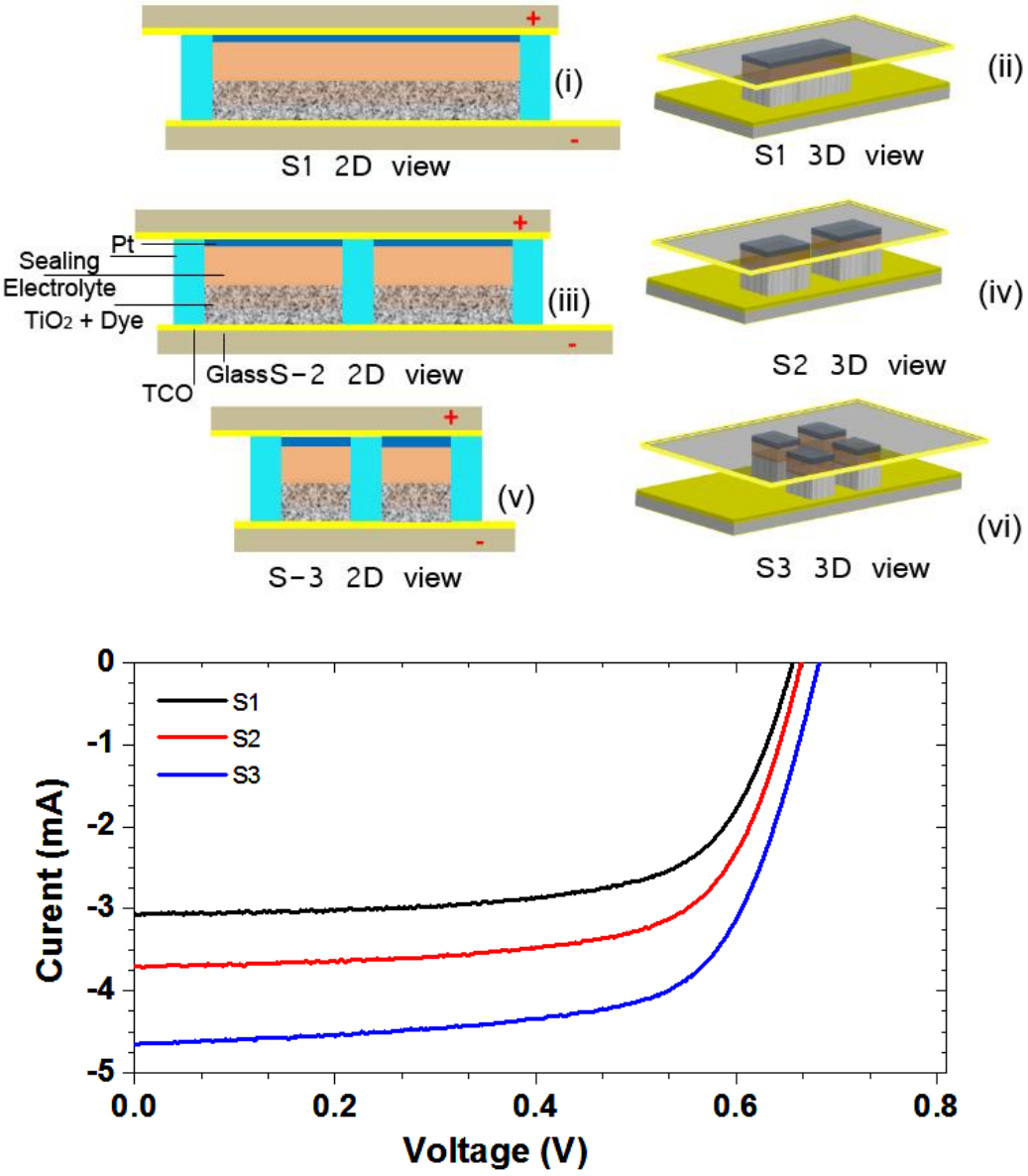

Figure 15: (a) Schematic of stacked cells on a single substrate and (b) IV curve of the three DSCs. Figures adapted from reference[157].

Table 4: Comparison of photovoltaic parameters of the three devices (S1 – S3). The parameters are calculated by considering the active area (28 mm^2), and aperture area (28, 28.8, and 30.28 mm^2 for S1, S2 and S3 respectively). Reproduced from reference [157].

Device design	Dimensions & active area (cm^2)	I_{SC} (mA)	J_{SC} (mA/cm^2)	V_{OC} (V)	FF	η_1 % (active area)	η_2 % (aperture area)
Single (S1)	~0.28	3.11	10.67	0.66	0.701	5.01	5.01
Split (S2)	~0.14 × 2 = 0.28	3.70	13.21	0.67	0.678	6.06	5.87
Split (S3)	~0.07 × 4 = 0.28	4.65	16.21	0.67	0.644	7.32	6.88

These studies show that the L_n alone as a device parameter has limitations to describe the collection of photoelectrons in large area DSCs and a three-dimensional analogue, such as the diffusion volume (V_n), is suggested to be a possible alternative. In the designed experiment of ref [157] (where three photoelectrode are of similar active volume but in different device designs as shown in Figure 15a), it was shown that restricting the diffusion pathways in three dimensions by appropriate device designs resulted in enhanced J_{SC} and η in photoelectrode of similar active volume (Figure 15b). Upon increasing the photoelectrode area, the competition between τ_n and τ_d becomes crucial. Given the τ_n of few milliseconds, the photoelectrons beyond a limit are never collected due to their longer τ_d. A ~20% greater charge collection efficiency (η_{cc}) in those designs was demonstrated by considering V_n which resulted in overall enhanced η; $\eta = f(\alpha, \phi_{in}, \phi_{reg}, \eta_{cc})$. The α (absorption coefficient), the ϕ_{in} (injection efficiency) and the ϕ_{reg} is the dye-regeneration efficiency are same in all the devices as they are made of similar materials and of similar photoelectrode thickness (~14 μm).

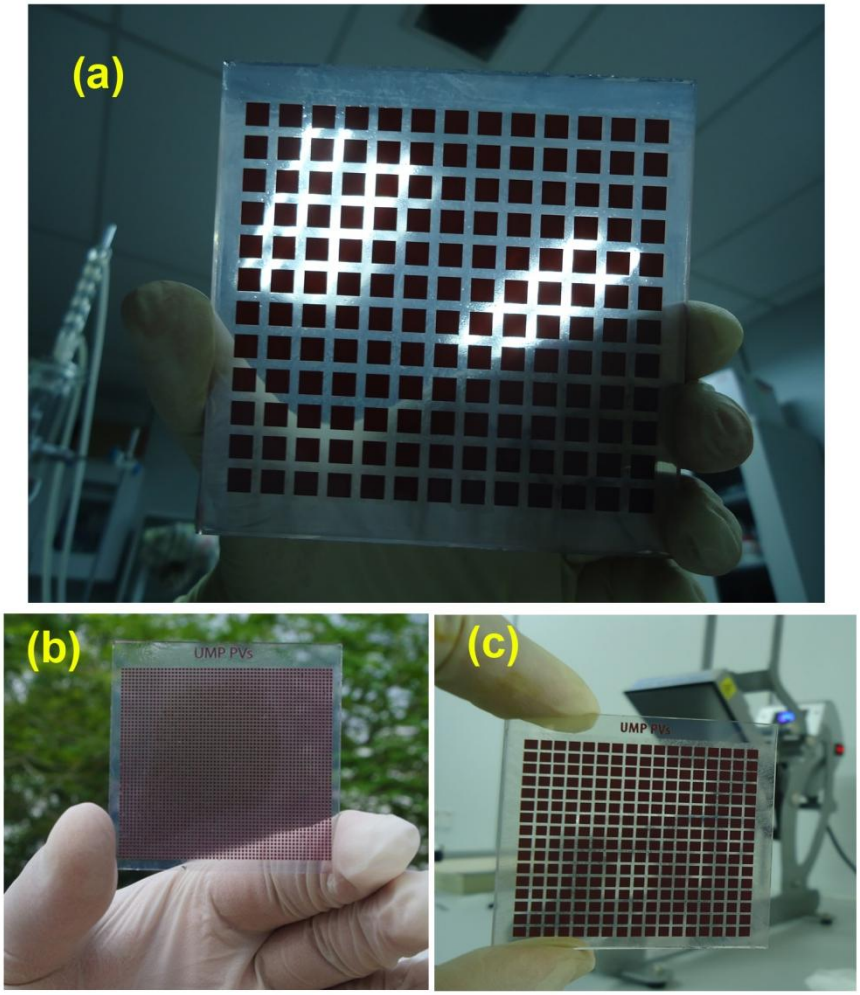

Figure 16: (a) A DSM photoelectrode (100 cm^2) printed at the Nanostructured Renewable Energy Materials Laboratory, Faculty of Industrial Sciences & Technology, Universiti Malaysia Pahang laboratory with individual cell dimensions are 0.5 cm x 0.5 cm with 2 mm interspacing, (b) a 25 cm^2 printed electrode with tiny dots of 1 mm^2 and interspacing of ~0.3 mm, and (c) is a 25 cm^2 photoelectrode with individual cell size of 4 mm^2 and an interspacing of ~1mm.Such designs are expected to yield very high J_{SC} or V_{OC} depending on the type of interconnection.

Based on our insights on photoanode area dependent DSC performance, we tested various module designs, where each unit cell consists of 1– 100 mm^2. We note that such split designs are likely to add difficulty in fabrication process as sealing and interconnection of individual cell will become a major issue. However, such designs have greater success possibility in *s*-DSMs as difference in concentration of the redox species between the

neighboring cells do not arise in solid electrolytes. Based on the connection types, these cells are likely to provide very high photocurrent or photovoltage in DSMs.

An alternative to avoid lateral diffusion and improve the η_{cc} could be the use of vertically aligned one-dimensional structures such as nanowires or nanotubes that would keep constant values of J_{SC} even with increased electrode area. Unfortunately up to now, the use of this kind of nanostructures in small area DSCs has not reported comparable J_{SC} values with respect to nanocolloidal films due to their lower roughness and thus dye uploads.

11. Stability test of DSMs

For DSC technology to be commercially successful, their long term performance under the device working conditions such as high temperature, humidity, and continuous light illumination are to be ensured. Commercial deployment of DSCs requires device working performance without a significant degradation for >10 years,[168] especially when its contenders, i.e., silicon PVs perform ~25 years with >80% of original η retained. Here we separately discuss the stability of (i) various components of DSC such as dye and electrolyte and (ii) outdoor long term stability of DSMs.

11.1. Thermal stability of dyes and electrolytes

The DSCs' organic materials are known to suffer high degradation rates when exposed to ambient conditions.[169] Also, liquid electrolyte causes leaking and corrodes the metallic grids used for interconnections if not properly encapsulated. In DSCs, the stability is primarily associated to the hermetic sealing: (i) the sealants should be stable at high temperature, (ii) passive to liquid electrolytes, and (iii) in case of spot sealing failure (pinholes), the materials chosen for grids should be resistant to corrosion and design should be robust enough to avoid spreading of the electrolyte out of the cell compartment.

The ECN started the Joule program (LOTS-DSC JOR3-CT98-0261) to realize the device outdoor performance capability for ~10 years.[170, 171] They investigated DSCs stability under intensive light (2.5 sun) and also thermal stability at temperatures up to 80 ^{o}C. Their master plate design using surlyn spacer with η ~5 – 6% showed stability up to 8300 h at 2.5 sun; a time equivalent to ~10 years outdoor operation. The η decreased <10% for 2000 h operation at 60 ^{o}C; which at 80 ^{o}C was 30%.[49] Such thermal stability is achieved by chemically changing the iodide/triiodide based electrolyte composition via addition of MgI_2 and CaI_2. The higher temperature induces instability to (i) the dye molecules by detaching it from the TiO_2 surface,[172] and (ii) the electrolyte components such as *tert*-butyl pyridine(TBP) and lithium iodide (LiI) during thermal aging.[49] To improve the high temperature stability of dyes, co-grafting it with 1-decylphosphnic acid (1-DPA) or hexadecylmalonic acid (HDMA) is suggested as a possible remedy.[173, 174] Although the above procedure improved the integrity of the dye–TiO_2 surface the additional dilution reduced amount of dye-anchoring and light harvesting thereby. On the other hand, the major advancement in electrolyte stability is reported by Grätzel *et al*.[172] who introduced a low volatile robust electrolyte in conjunction with an amphiphilic ruthenium sensitizer (K19). In their study ~8.2% efficient DSCs retained 98% of the original performance after soaking 1000 h at 60 ^{o}C in light. Thermal stability of the above dye – TiO_2 conjugate was further verified at 80 ^{o}C in dark. Through these studies, for the first time, the DSCs achieved the specifications laid out for outdoor performance of silicon solar cells.

A significant advancement in the DSCs' performance at temperature >80 ^{o}C is reported by Dyesol Ltd. By employing stable dyes (N709 and Y123) and 3-methoxypropionitrile (MPN) based electrolyte, the DSCs showed stability over 90% for 1000 h at 95 ^{o}C.[91] The major contributor to the observed ~10% drop in η is from the V_{OC}

originating from change in concentration of the redox species in the electrolyte. Other photovoltaic parameters (J_{SC} and FF) showed no notable degradation. These results are encouraging and open the possibility that DSC technology can be deployed in extremely hot places.

The substitution of Surylin by other more stable sealants such bynel (EPFL), frits (ECN) or UV-cured epoxy composite sealants (Dyesol) has been a key point in these advancements. Surylin starts softening at 70ºC what makes it unsuitable for high temperature applications and is permeable to water, what may cause long term problems of stability.

11.2. Long term stability of DSMs

Only few studies are reported on stability of DSMs so far. In general, stability of DSMs is inferior to its laboratory counterparts. In 2004, a research group of AISIN SEIKI carried out the first outdoor stability testing of DSMs (64 serially connected cells of 10×10 cm^2) for over half an year.[108] Surprisingly, no significant effect of moisture on device performance was noticed. They reported that a DSM generated comparatively more electricity than silicon based cell over an year due to (i) DSMs' superior performance in low light; (ii) improved rheology of the electrolyte at higher temperatures and (iii) their less dependence on angle of light incidence. The devices showed ~20% drop in output power after one year of operation although the source of this drop was not elaborated except the leakage of the electrolyte in few cells. This drop was overcome in an extended investigation using a set of experimental techniques to figure out the contribution from each component of DSMs on its performance degradation.[103] This study showed remarkable results for a long term (2.5 years) outdoor stability: (i) no leakage of the electrolyte was found out in the device, (ii) the dye (N719) and the carbon counter electrode were stable as confirmed by Raman spectroscopy and stable J_{SC}. However, the concentration of triiodide is still reduced in the

electrolyte.. This effect has been attributed to irreversible reactions of iodide and iodine species with water present in the electrolyte such leading to the bleaching of the electrolyte and the irreversible formation of IO_3^-.[175, 176]

$$\begin{aligned} 3I_3^- + 6OH^- &\leftrightarrow IO_3^- + 3H_2O + 8I^- \\ I^- + 6OH^- + 6h^+ &\leftrightarrow IO_3^- + 3H_2O \\ 3I_2 + 3H_2O &\leftrightarrow IO_3^- + 6H^+ + 5I^- \end{aligned} \quad (2)$$

These reactions have been shown to be enhanced by UV light and temperature.[176,177] Bleaching of electrolyte is also dependent of electrolyte solvent and its origin, not clearly stated yet, associated to TiO_2-electrolyte or TiO_2-dye-electrolyte interactions.[178] Good sealing and low humidity conditions during the fabrication process are then required to obtain good long term stability results.

Towards the thermal stability testing of DSMs, a report by Kroon *et al.*[179] of ECN showed significantly stable (80%) performance at >80 ^oC for 3000 h. The devices showed ~20% decrement in output power using robust electrolyte. In another study by Mastroianni *et al.*[99] the stability of DSMs (30 cells of area 3.6 cm^2) are tested in indoor (at AM 1.5 G and 85 ^oC) and outdoor (horizontally placed and titled at 25^o) conditions. For a period of 3200 h, the outdoor DSMs were significantly stable with only 10% fall in its original efficiency. However, the vertically placed outdoor cells showed higher degradation at maximum power point due to uneven triiodide concentration indicating that the vertical orientation of *l*-DSMs affect the device lifetime. A detailed impedance characterization also revealed reduction in the diffusion length and a possible alteration at TiO_2/electrolyte interface.

Asghar *et al.*[169] summarized the major instability issues in a recent review and suggested that (i) Z709 and K19 are the only stable dyes at temperature ~80 ^oC and (ii) devices mostly employing polymer and ionic liquid electrolytes passed light soaking test (60

^{o}C) and thermal stress test (80 ^{o}C) for 1000 h. Although significant advancements are made towards the stability investigation on DSC and DSMs, nevertheless, such reports were only limited to glass substrate based devices. Stability of flexible DSCs/DSMs at temperature >50 ^{o}C temperatures is yet to be investigated although they have shown considerable stability until 50 ^{o}C.[180] Furthermore, a standard criterion is needed to be set to investigate stability as the device undergoes chemical changes when exposed to outdoor conditions; and therefore, chemical investigations along with electrical characterizations are essential while reporting the stability analysis.

The design of DSMs introduces a larger complexity than the simpler DSCs and consequently, sealing process becomes more difficult. To avoid that a failure in a single point of the sealing ruins the performance of a complete module, it is needed that the external components that may be affected by direct contact with leaking electrolyte do not degrade. Of particular importance are the collecting grids; silver should be avoided in the most exposed sections of the cells as iodide reacts very efficiently with it. Alternative materials for collecting electrodes may be Carbon, Titanium or Tin (at cathode).

Robust module designs must contemplate ways to control or neutralize the occurrence of a localized escape of electrolyte. The use of gellified electrolytes[181,182] or solid electrolytes or double sealing structures (Fujikura) may help to avoid the loss of electrolyte and thus improve module performance.

11.3. Reverse bias degradation of DSMs

With respect to single cells, stability of modules is made considerably more complex by the fact that large areas increase the probability of disuniformities and defects which can lead to increase degradation rates or failures (e.g. non uniform coverage or pinholes in the encapsulation or interconnections). Furthermore, when cells are connected together in series

in a module, the possibility of the occurrence of reverse bias degradation effects must be considered. In fact, a cell that is electrically mismatched in a module, which occurs when it is shadowed or has degraded at a higher rate compared to other cells, can become inversely polarized by the other well-performing cells of the system.[146] Current is then forced though it by the other cells. Over the long term, this can lead to device degradation and even failure.[183] Contributing to reverse bias degradation are triiodide depletion and the presence of impurities, in particular water. Gaining a further understanding of reverse bias phenomena, acting upon these components and setting up diode protection strategies is important for delivering long-lasting DSMs.[184]

12. Standards for DSMs

Except for some exceptions, due to the relative infancy of industrial development, reports on systematic statistical long term testing outdoors are also scant. At the moment stability testing on DSMs has involved protocols developed for thin films. Even if more statistics and continued tests are required, some promising developments have been reported. The DSMs have passed thermal stability testing (IEC 1215) but still with its η decreased by 30–40%. Fujikura have shown cells and submodules that have passed several endurance tests according to JIS C 8938 standards.[185] Dyepower has shown successful UV preconditioning, humidity freeze and damp heat IEC 61646 tests carried out over large area (> 500 cm^2) DSC modules.[186] The IEC tests are meant only for indoor analysis and do not consider the chemical changes that DSMs undergo upon exposure to atmospheric conditions. For DSMs, a different set of standards are required that analyze the device performance close to the natural outdoor conditions and should also involve chemical changes such as UV-stability and chemical stability under atmospheric conditions.

For DSMs to be a successful commercial product, it has to pass few standards which are widely applied on silicon and thin film solar cells such as IEC 61646, IEC 1215, IEC 1646, and IEC 1215. These standards are necessary to predict sufficient stability of the device and assurance of the lifetime required. Test protocols tailored for DSC technology have yet to be designed and implemented. Besides, there is also a need to set standards for DSM fabrication and characterization because different fabrication techniques and experimental conditions result in significant variation in η (sections 5 – 9). A similar standardization is suggested by Yang *et al*.[187] for laboratory scale DSCs for their reliable evaluation such as the calibration of the solar simulator via reference cells, the measurement time of the photovoltaic characterizations (I-V & incident photon-to-current conversion efficiency), and the masking process. Nevertheless, absence of such standards in DSMS leads to misconceptions, particularly, while reporting module efficiency values: a number of researchers reported η with respect to active area while few other reported with respect to active and aperture area. Ultimately, the latter is the most important number. In fact, since aperture ratios (the ratio between active and aperture areas) can differ greatly depending on the methods of construction, the performance on active area and aperture area of DSMs can differ significantly. In fact, in the literature aperture ratios vary from 85%,[84] to less than 50%,[141] so that η drops between 85% and less than half of the reported active area value when total area is considered. It is important that both numbers are given.

13. Conclusions and Future Projections

Any PV technology entering the market has been usually pitched against three main parameters: (a) efficiency, (b) lifetime and (c) cost. Over 80% of the current market is cornered by silicon cells which thus remains the benchmark for PV systems. Over the last few years the price of silicon modules has decreased considerably. In fact, the drop has been

so significant that in 2012 the average cost of modules came below the significant threshold of 1$/Wp (i.e. ~0.8 $/Wp).[188] While part of this is due to oversupply in the market, a good portion is also due to advances in technology and economies of scale due to an increase in cumulative worldwide PV production. Thus, whereas a decade ago new technologies may have aimed at also competing on cost calculated in $/Wp, even when considering initial markets, today a more suitable roadmap considers seeking applications where the new technology offers competitive advantages in functionality over silicon or other existing PV technologies. In Figure 17, we have added a technological "functionality" entry to the competitive mix in which DSM must compete.

Figure 17 can help identify entry or niche markets products (each with a different mix of the 3 parameters and associated technological functionalities) to which particular DSM technology development can be focused. Subsequently, with continued R&D development the market space will grow, economies of scale will also kick-in so that, in the longer term, the technology may enter even the more conventional PV system arena. Capital cost to implement industrial fabrication of DSMs is another advantage of this technology as required investments are one order of magnitude smaller than standard technologies. The roadmap for the technological development of DSMs depends strongly on the application. This is also the reason why different designs and architectures for DSMs are being explored (e.g. glass, flexible, liquid based, solid state, monolithic, double plate Z, W or parallel etc).

Figure 17: Scheme representing inter-relations between the three parameters (power conversion efficiency, stability and cost) which must be considered, together with functionality, for a successful industrial product development for dye solar cell modules. Different applications and markets lead to different mix of requirements and thus different DSM technological development (e.g. glass, flexible, material combinations, device architecturesetc).

Although there are many commercial developers of materials and technology working on various aspects of DSMs and prototypes, the market where actual commercial products are available integrating DSMs in retail products (at the time of writing), is represented by electronic products, especially those for portable or indoor environments.[19] G24 Power Ltd is a provider of DSMs for these applications, which are made with flexible titanium foil working electrodes and plastic/ITO counter electrodes and are series connected.

Due to their remarkable performance under low levels of light and compact fluorescent lamps, there is strong interest both for glass based products (http://ricoh.com/release/2014/0611_1.html) and even more so for thin flexible DSMs (www.gcell.com) which can be easily integrated in fixed or portable electronic products such as sensors in the home and personal computer peripherals. Although efficiencies of these

flexible modules are still not particularly high under STC, their power output has been shown to outperform competing technologies, including amorphous silicon (the current most suitable technology) under indoor lighting.[18] The commercialization of these products with integrated DSMs has been enabled by the fact that efficiencies are particularly high at indoors, their flexibility and light weightness permit easy integration (and portability), degradation rates are reduced in less-harsh indoor conditions and lifetimes of few years (similar to that of the electronic product they are integrated on) are commercially acceptable. The DSMs, in this particular arena, thus deliver functionality which conventional crystalline silicon does not. The cost here is not measured in $/Wp but in the added value their integration brings (eg. eliminating the need to replace batteries). The development roadmap for flexible devices involves continuing to diminish costs (opening up the possibility of integrating the devices in cheaper products), increasing lifetimes even outdoors (for portable or semi-fixed/protable installations) by researching more performing (and cheaper) material combinations and encapsulation barrier strategies. Furthermore, the development of efficient hole blocking compact layers at the working electrode is particularly important under low levels of illumination.

A huge market for DSMs is represented by BIPV where devices can be incorporated into big installations worth hundreds of millions of dollars globally. Development work is ongoing by various industrial entities (see Table 2) to produce prototypes and demonstrators for integration in applications such as bus shelters, roofing and building facades, including semi-transparent windows.[189] The latter is particularly suited for DSMs because most of the technology development has been carried out on glass. Glass has also exceptional barrier properties (which is crucial for lifetimes) and is becoming ever more a widespread material for modern buildings. For integration in shelters, lifetimes of a few years can suffice.

However integration in buildings requires very challenging lifetimes of over 15-20 years. The competitive advantage glass DSM technology brings, is that of enabling the power-generating unit to be semitransparent.[190] In fact the transparency versus efficiency of the DSM can be tuned depending on the requirements for energy generation, visible light transmission and its color.[17] For properly rating glass facade applications, the efficiency parameter at STC should be at least complemented by other parameters such as energy produced over the course of the year in real environmental conditions,[191] which depends greatly on location, both geographic and related to the building (e.g. vertical or tilted conditions). DSMs have been shown to deliver 10-20% more energy (at the same power rating) compared to silicon installations (even though efficiencies still remain significantly lower).[108] For BIPV applications, perfecting encapsulation, developing more stable dyes, less volatile electrolytes with stabilizing additives, quasi or fully solid-state carrier mediators are paths followed by researchers to improve stability. For large scale installations, the uniformity and tolerances that can be achieved in the manufacturing process over (very) large areas, together with the management of the electrical output power of the modules (and panels), are important and complex issues to be tackled. The most suitable device architecture can depend on the size of the unit module which makes up the panel. Either parallel or series or combined interconnections can be selected to deliver the required voltage and current levels. Electrical and diode protection strategies will also differ depending on the type and size of the module. For BIPV, as much as the $/Wp, it is important to consider the marginal added costs with respect to conventional building material (e.g. the cost of a façade with PV functionality compared to that without). Much of the engineering work to bring efficiency, stability and costs to the levels required by the BIPV industry, together with the peculiar functionality of DSMs required by the markets, is being carried out, often "quietly" in industrial R&D divisions and results and developments are only partly publicly available. The growing

activity in patent filing in this field shows (see Figure 6a), however, that intense work is being carried out to bring the technology to market and, at the same time, that there are tremendous opportunities for exciting innovation in the field.

While an immense research is carried out on improving laboratory scale DSCs, a little focus is given to their large area devices: research on DSMs is ~1% of that on DSCs. Due to this negligence, the η in the DSMs showed comparatively little improvement since their first report (5.6% in 1996). The maximum reported in the DSMs is 8.2% through optimized front and back illumination, which is still significantly lower than that obtained in high efficiency single cells (~13%). Little attention towards device engineering and a complete negligence of charge transport in DSMs are the main factors behind the comparatively lower performance of DSMs.

Acknowledgments

This work was financially supported by the ministry of higher education Malaysia through prototype research grant scheme. We also acknowledge support by a project from Generalitat Valenciana (ISIC/2012/008). We are thankful to David Martineau of Solaronix Ltd, Damion Milliken of Dyesol Ltd. for the sharing of information on comparative performance of DSMs Vs others, and also to Iván Mora Seró for discussion on DSC cost analysis. The authors also thank to Dr Hans Desilvestro of Dyesol for useful discussion 'route to DSMs' future'.

Bibliography

Azhar Fakharuddin obtained his bachelor's degree in electronic engineering from Mehran University of Engineering & Technology, Pakistan and Master's degree in electronic engineering from Universiti Malaysia Pahang (UMP). He is currently pursuing doctoral research at the Nanostructured Renewable Energy Materials Laboratory of UMP on the scalability issues of dye-sensitized solar cells (DSCs). His work is primarily focused on investigation of the charge transport parameters while up scaling DSCs and to explore appropriate device designs and materials architectures to improve charge collection efficiency in large area photoelectrodes. His research interests also include synthesis and characterization of metal oxide semiconductors for organic photovoltaics particularly dye and perovskite sensitized solar cells/modules. Email: clife03@yahoo.com

Rajan Jose is a Professor of Materials Science and Engineering at the Faculty of Industrial Sciences and Technology, Universiti Malaysia Pahang (UMP). He supervises the Nanostructured Renewable Energy Materials Laboratory in the UMP. He conducted his doctoral research at the Council of Scientific and Industrial Research (CSIR), Trivandrum, India and received PhD degree in the year 2002 for his work on nanostructured perovskite ceramics for microwave and superconducting electronics. He has worked at various capacities at the Indira Gandhi Centre for Atomic Research (India), AIST (Japan), Toyota Technological Institute (Japan), and the National University of Singapore (Singapore) before joining UMP. He has published over 100 papers in SCI journals. He holds over 20 patents nationally and internationally. His h-index is 29 and g-index is 50 currently. His research interests include nanostructured materials and renewable energy devices. E-mail: rjose@ump.edu.my / joserajan@gmail.com

Thomas M. Brown investigated polymer OLEDs for his PhD at the Cavendish Laboratory, University of Cambridge. From 2001-2005 he developed E-paper as Senior Engineer with Plastic

Logic Ltd. In 2005 he was recipient of a "Re-entry" Fellowship awarded by the Italian Ministry of Education, University and Research and is Associate Professor at the Department of Electronic Engineering, University of Rome-Tor Vergata. Cofounder of the Centre for Hybrid and Organic Solar Energy, his current research is in dye sensitized, perovskite, and polymer solar cells. He is on the Advisory Board of Dyepower and is author of over 100 publications including 16 patents. E-mail: thomas.brown@uniroma2.it

Francisco Fabregat-Santiago is Associate Professor at Physics department of Universitat Jaume I de Castelló (Spain). He is an expert in electro-optical characterization of devices and particularly known by his works in the use of the impedance spectroscopy to model, analyze and interpret the electrical characteristics (charge accumulation, transfer reactions and transport) of devices and films including ZnO and TiO2 nanostructured films (nanocolloids, nanorods and nanotubes), dye sensitized and quantum dot solar cells, electrochromic materials and liquid and solid state hole conductors. His latest research is focused on perovskite solar cells, photoinduced water splitting, microbial fuel cells and bio-sensors. He has published 85 papers that accumulate more than 4000 citations with an index h = 31. Email: fran.fabregat@fca.uji.es

Juan Bisquert is a professor of applied physics at Universitat Jaume I de Castelló, Spain (http://www.elp.uji.es/jb.php). He conducts experimental and theoretical research on nanoscale devices for production and storage of clean energies. His main topics of interest are materials and processes in perovskite solar cells, nanostructured solar cells, solar fuel production, and lithium battery. He has developed the application of measurement techniques and physical modeling of nanostructured energy devices that relate the device operation with the elementary steps taking place at the nanoscale dimension: charge transfer, carrier transport, chemical reaction, etc., especially in the field of impedance spectroscopy, as well as general device models. He authored 280 peer reviewed

papers, h-index 53, and is currently a Senior Editor of the Journal of Physical Chemistry, and member of Editorial Board of Energy and Environmental Science, and ChemElectroChem. E-mail: bisquert@fca.uji.es

References

(1) Key World Energy Statistics, http://www.iea.org/publications/freepublications/publication/KeyWorld2013.pdf (accessed December 2013) .

(2) Grätzel, M. *Acc. Chem. Res.* 2009, **42**, 1788-1798.

(3) Perez, R.; Zweibel, K.; Hoff, T. E. *Energy Policy* 2011, **39**, 7290-7297.

(4) Nelson J, E. C. *Phil. Trans. R. Soc. A* 2013, **371**, 4.

(5) Docampo, P.; Guldin, S.; Leijtens, T.; Noel, N. K.; Steiner, U.; Snaith, H. J. *Adv. Mater.*, 2014.

(6) Solar generation PV capacity, http://www.bp.com/en/global/corporate/about-bp/statistical-review-of-world-energy-2013/review-by-energy-type/renewable-energy/solar-energy.html, (accessed January 2014).

(7) Wirth, H. http://www.ise.fraunhofer.de/en/publications/veroeffentlichungen-pdf-dateien-en/studien-und-konzeptpapiere/recent-facts-about-photovoltaics-in-germany.pdf, ((accessed November 2013).

(8) ZSW press release, http://www.zsw-bw.de/uploads/media/pi18-2013-ZSW-WorldrecordCIGS.pdf, (accessed December 2013).

(9) NREL: Best research cell efficiencies, http://www.nrel.gov/ncpv/images/efficiency_chart.jpg, (accessed May 2014).

(10) First Solar, http://www.firstsolar.com/Innovation/Advanced-Thin-Film-Modules, (accessed December 2013).

(11) Hardin, B. E.; Snaith, H. J.; McGehee, M. D. *Nat. Photon.* 2012, **6**, 162-169.

(12) British Petroleum review, bp.com/statisticalreview , (accessed November 2013).

(13) IEA, http://www.worldenergyoutlook.org/media/weowebsite/2012/PresentationtoPress. pdf, (accessed January 2014).

(14) Grätzel, M. *J. Photochem. Photobiol.* 2003, **4**, 145-153.

(15) Hagfeldt, A.; Boschloo, G.; Sun, L.; Kloo, L.; Pettersson, H. *Chem. Rev.*, 2010, **110**, 6595-6663.

(16) Bisquert, J. *ChemPhysChem*, 2011, **12**, 1633-1636.

(17) R. Tagliaferro, D. Colonna, T. M. Brown, A. Reale and A. Di Carlo, *Opt. Express*, 2013, **21**, 3235-3242.

(18) N. Sridhar and D. Freeman, Proceedings of 26th European Photovoltaic Solar Energy Conference and Exhibition, hamburg, Germany, 2011.

(19) Brown T. M., De Rossi F., Di Giacomo F., Mincuzzi G., Zardetto V., Reale A. and Di Carlo A., *Journal of Materials Chemistry A*, 2014, **2**, 10788-10817.

(20) Wang, Q.; Ito, S.; Grätzel, M.; Fabregat-Santiago, F.; Mora-Seró, I.; Bisquert, J.; Bessho, T.; Imai, H. *J. Phys. Chem. B*, 2006, **110**, 25210-25221.

(21) J. Bisquert, *PCCP*, 2008, **10**, 49-72.
(22) Halme, J.; Vahermaa, P.; Miettunen, K.; Lund, P. *Adv. Mater.* 2010, **22**, E210-E234.
(23) Boschloo, G.; Hagfeldt, A. *Acc. Chem. Res.*, 2009, **42**, 1819-1826.
(24) Daeneke, T.; Kwon, T. H.; Holmes, A. B.; Duffy, N. W.; Bach, U.; Spiccia, L. *Nature Chem.*, 2011, **3**, 211-215.
(25) Liu Y., Jennings J. R., Huang Y, Wang Q, Zakeeruddin S. M., and Grätzel M., *J. Phys. Chem. C*, 2011, **115**, 18847-18855.
(26) Mathew, S.; Yella, A.; Gao, P.; Humphry-Baker, R.; Curchod, B. F. E.; Ashari-Astani, N.; Tavernelli, I.; Rothlisberger, U.; Nazeeruddin, M. K.; Grätzel, M. *Nature Chem.*, 2014, **6**, 242-247.
(27) Yamaguchi, T.; Tobe, N.; Matsumoto, D.; Nagai, T.; Arakawa, H. *Sol. Energy Mater. Sol. Cells*, 2010, **94**, 812-816.
(28) Green, M. A.; Emery, K.; Hishikawa, Y.; Warta, W.; Dunlop, E. D. *Progress in Progr. Photovolt.: Res. Appl.*, 2014, **22**, 1-9.
(29) R. Harikisun and H. Desilvestro, *Solar Energ.*, 2011, 85, 1179-1188.
(30) D. Bari, N. Wrachien, R. Tagliaferro, T. M. Brown, A. Reale, A. Di Carlo, G. Meneghesso and A. Cester, *Microelectronics Reliability*, 2013, 53, 1804-1808.
(31) Xiong, D.; Chen, W. *Front. Optoelectron.*, 2012, **5**, 371-389.
(32) Im, J. H.; Lee, C. R.; Lee, J. W.; Park, S. W.; Park, N. G. *Nanoscale*, 2011, **3**, 4088-4093.
(33) Castelli, I. E.; Olsen, T.; Datta, S.; Landis, D. D.; Dahl, S.; Thygesen, K. S.; Jacobsen, K. W. *Energ. Environ. Sci.*, 2012, **5**, 5814-5819.
(34) Carnie, M. J.; Charbonneau, C.; Davies, M. L.; Troughton, J.; Watson, T. M.; Wojciechowski, K.; Snaith, H.; Worsley, D. A. *Chem. Comm.*, 2013, **49**, 7893-7895.
(35) Kim, H. S.; Lee, J. W.; Yantara, N.; Boix, P. P.; Kulkarni, S. A.; Mhaisalkar, S.; Grätzel, M.; Park, N. G. *Nano Lett.*, 2013, **13**, 2412-2417.
(36) Park, N. G. *J. Phys. Chem. Lett.*, 2013, **4**, 2423-2429..
(37) You, J.; Hong, Z.; Yang, Y.; Chen, Q.; Cai, M.; Song, T.-B.; Chen, C.-C.; Lu, S.; Liu, Y.; Zhou, H. *ACS Nano*, 2014, **8**, 1674–1680.
(38) Hao F., Stoumpos C. C., Cao D. H., Chang R. P. H., Kanatzidis M. G., *Nature Photon.*, **2014**.
(39) Matteocci F., S. Razza, F. Di Giacomo, S. Casaluci, G. Mincuzzi, T. M. Brown, A. D'Epifanio, S. Licoccia and A. Di Carlo, *PCCP*, 2014, 16**,** 3918-3923.
(40) Seo J., Park S., Chan Kim Y., Jeon N. J., Noh J. H., Yoon S. C. and Seok S. I., *Energ. Environ. Sci.*, 2014.
(41) Ubertini, S.; Desideri, U. *Renew. Energ.*, 2003, **28**, 1833-1850.
(42) Dyesol, http://www.dyesol.com/about-dsc/advantages-of-dsc , Accessed 13 December 2013, 2013.
(43) K. Kalyanasundaram, *Dye-sensitized Solar Cells*, CRC press, Switzerland, 1 edn., 2010.
(44) Zardetto, V.; Mincuzzi, G.; De Rossi, F.; Di Giacomo, F.; Reale, A.; Di Carlo, A.; Brown, T. M. *App. Energ.*, 2014, **113**, 1155-1161.
(45) H. Arakawa, T. Yamaguchi, T. Sutou, Y. Koishi, N. Tobe, D. Matsumoto and T. Nagai, *Curr. Appl. Phys.*, 2010, **10**, S157-S160.
(46) Zardetto, V.; Di Giacomo, F.; Garcia-Alonso, D.; Keuning, W.; Creatore, M.; Mazzuca, C.; Reale, A.; Di Carlo, A.; Brown, T. M. *Adv. Energ. Mater.*, 2013, **3**, 1292-1298.

(47) Berginc M., Opara Krašovec U., Jankovec M. and Topič M., *Sol. Energy Mater. Sol. Cells*, 2007, **91**, 821-828.

(48) A. Hinsch, J. M. K., R. Kern, I. Uhlendorf, A. Meyer, J. Holzbock, J. Ferber *Prog. Photovolt: Res. Appl.*, 2001, **9**, 425-438.

(49) Sommeling, P. M.; Späth, M.; Smit, H. J. P.; Bakker, N. J.; Kroon, J. M. *J. Photochem. Photobiol.*, 2004, **164**, 137-144.

(50) (Skoplaki, E.; Palyvos, J. A. *Sol. Energ.*, 2009, **83**, 614-624.

(51) Ray, K. L., Bachelor of Science Thesis, Massachusetts Institute of Technology, 2010.

(52) Kalowekamo, J.; Baker, E. *Sol. Energ.*, 2009, **83**, 1224-1231.

(53) Tanabe N., Fujikura Tech. Rev., 2010.

(54) Powell, D. M.; Winkler, M. T.; Choi, H. J.; Simmons, C. B.; Needleman, D. B.; Buonassisi, T. *Energ. Environ. Sci.*, 2012, **5**, 5874-5883.

(55) Beiley, Z. M.; McGehee, M. D. *Energ. Environ. Sci.*, 2012, **5**, 9173-9179.

(56) Azzopardi, B.; Emmott, C. J. M.; Urbina, A.; Krebs, F. C.; Mutale, J.; Nelson, *Energ. Environ. Sci.*, 2011, **4**, 3741-3753.

(57) Hashmi, G.; Miettunen, K.; Peltola, T.; Halme, J.; Asghar, I.; Aitola, K.; Toivola, M.; Lund, P. *Renew sust. energ. rev.*, 2011, **15**, 3717-3732.

(58) Ip, A. H.; Thon, S. M.; Hoogland, S.; Voznyy, O.; Zhitomirsky, D.; Debnath, R.; Levina, L.; Rollny, L. R.; Carey, G. H.; Fischer, A.; Kemp, K. W.; Kramer, I. J.; Ning, Z.; Labelle, A. J.; Chou, K. W.; Amassian, A.; Sargent, E. H. *Nature Nanotech.*, 2012, **7**, 577-582.

(59) Toby Meyer, M. S., Asef Azam, David Martineau, Frédéric Oswald, Stéphanie Narbey, Grégoire Laporte, Robin Cisneros, Giulia Tregnano, Andreas Meyer, CleanTechDay 3rd Generation Photovoltaics, CSEM. Basel, 2009.

(60) Kay, A.; Grätzel, M. *Sol. Energy Mater. Sol. Cells*, 1996, **44**, 99-117.

(61) Pettersson, H.; Nonomura, K.; Kloo, L.; Hagfeldt, A. *Energ. Environ. Sci.*, 2012, **5**, 7376-7380.

(62) Benson, D. K.; Branz, H. M. *Sol. Energy Mater. Sol. Cells*, 1995, **39**, 203-211.

(63) Zhou, H.; Song, T. B.; Chung, C. H.; Lei, B.; Bob, B.; Zhu, R.; Duan, H. S.; Hsu, C. J.; Yang, Y. *Adv. Energ. Mater.*, 2012, **2**, 1368-1374.

(64) López-López, C.; Colodrero, S.; Calvo, M. E.; Míguez, H. *Energ. Environ. Sci.*, 2013, **6**, 1260-1266.

(65) Xie, Z.; Jin, X.; Chen, G.; Xu, J.; Chen, D.; Shen, G. *Chem. Comm.*, 2014, **50**, 608-610.

(66) Wang, K.; Wu, H.; Meng, Y.; Zhang, Y.; Wei, Z. *Energ. Environ. Sci.*, 2012, **5**, 8384-8389.

(67) Wei, D.; Scherer, M. R. J.; Bower, C.; Andrew, P.; Ryhänen, T.; Steiner, U. *Nano Lett.*, 2012, **12**, 1857-1862.

(68) Thakur, V. K.; Ding, G.; Ma, J.; Lee, P. S.; Lu, X. *Adv. Mater.*, 2012, **24**, 4071-4096.

(69) Yang, S.; Zheng, J.; Li, M.; Xu, C. *Sol. Energy Mater. Sol. Cells*, 2012, **97**, 186-190.

(70) Shen, P. K.; Huang, H. T.; Tseung, A. C. C. *J. Electrochem. Soc.*, 1992, **139**, 1840-1845.

(71) Zhong, Q.; Dahn, J. R.; Colbow, K. *Phys. Rev. B*, 1992, **46**, 2554-2560.

(72) Cronin, J. P.; Tarico, D. J.; Tonazzi, J. C. L.; Agrawal, A.; Kennedy, S. R. *Sol. Energy Mater. Sol. Cells*, 1993, **29**, 371-386.

(73) Deepa, M.; Kar, M.; Agnihotry, S. A. *Thin Solid Films*, 2004, **468**, 32-42.

(74) Kumar, V.; Singh, N.; Kumar, V.; Purohit, L. P.; Kapoor, A.; Ntwaeaborwa, O. M.; Swart, H. C. *J. Appl. Phys.*, 2013, **114**, 134506-134506-6.

(75) Baetens, R.; Jelle, B. P.; Gustavsen, A. *Sol. Energy Mater. Sol. Cells*, 2010, **94**, 87-105.

(76) C. Bechinger, S. Ferrere, A. Zaban, J. Sprague and B. A. Gregg, *Nature*, 1996, 383, 608-610.

(77) Bechinger, C.; Gregg, B. A. *Sol. Energy Mater. Sol. Cells*, 1998, **54**, 405-410.

(78) Huang, L.-M.; Hu, C.-W.; Liu, H.-C.; Hsu, C.-Y.; Chen, C.-H.; Ho, K.-C. *Sol. Energy Mater. Sol. Cells*, 2012, **99**, 154-159.

(79) Ahn, K.-S.; Yoo, S. J.; Kang, M.-S.; Lee, J.-W.; Sung, Y.-E. *J. Pow. Sources*, 2007, **168**, 533-536.

(80) Maçaira, J.; Andrade, L.; Mendes, A. *Renew. Sust. Energ. Rev.*, 2013, **27**, 334-349.

(81) D. D'Ercole, L. Dominici, T. M. Brown, F. Michelotti, A. Reale and A. Di Carlo, *Appl. Phys. Lett.*, 2011, 99, -.

(82) Solaronix NEWS, http://www.solaronix.com/news/ccrdelivery/ (accessed January 2014).

(83) Dyesol NEWS, http://www.dyesol.com/partners/current-projects, (accessed December 2013).

(84) L. Han, A. Fukui, Y. Chiba, A. Islam, R. Komiya, N. Fuke, N. Koide, R. Yamanaka and M. Shimizu, *App. Phy. Lett.*, 2009, 94.

(85) Crossland, E. J. W.; Noel, N.; Sivaram, V.; Leijtens, T.; Alexander-Webber, J. A.; Snaith, H. J. *Nature*, 2013, **495**, 215-219.

(86) Hey, A. S.; Snaith, H. J. *J. App. Phys.*, 2013, **114**, 183105.

(87) Matteocci, F.; Casaluci, S.; Razza, S.; Guidobaldi, A.; Brown, T. M.; Reale, A.; Di Carlo, A. *J. Pow. Sources*, 2014, **246**, 361-364.

(88) Agarkar, S. A.; Dhas, V. V.; Muduli, S.; Ogale, S. B. *RSC Adv.* 2012, **2**, 11645-11649.

(89) Kang, J. G.; Kim, J. H.; Kim, J. T. *Int. J. Photoenerg.* 2013, 472086.

(90) Dyesol Media, http://www.dyesol.com/posts/cat/corporate-news/post/dyesol-achieves-technical-breakthrough/., (accessed December 2013).

(91) Jiang, N.; Sumitomo, T.; Lee, T.; Pellaroque, A.; Bellon, O.; Milliken, D.; Desilvestro, H. *Sol. Energy Mater. Sol. Cells*, 2013, **119**, 36-50.

(92) Pettersson, H.; Gruszecki, T.; Bernhard, R.; Häggman, L.; Gorlov, M.; Boschloo, G.; Edvinsson, T.; Kloo, L.; Hagfeldt, A. *Progr. Photovolt.: Res. Appl., Applications*, 2007, **15**, 113-121.

(93) S. Ito, T. N. Murakami, P. Comte, P. Liska, C. Grätzel, M. K. Nazeeruddin and M. Grätzel, *Thin Solid Films*, 2008, **516**, 4613-4619.

(94) Späth, M.; Sommeling, P. M.; Van Roosmalen, J. A. M.; Smit, H. J. P.; Van Der Burg, N. P. G.; Mahieu, D. R.; Bakker, N. J.; Kroon, J. M. *Progr. Photovolt.: Res. Appl., Applications*, 2003, **11**, 207-220.

(95) Sastrawan, R.; Beier, J.; Belledin, U.; Hemming, S.; Hinsch, A.; Kern, R.; Vetter, C.; Petrat, F. M.; Prodi-Schwab, A.; Lechner, P.; Hoffmann, W. *Sol. Energy Mater. Sol. Cells*, 2006, **90**, 1680-1691.

(96) Dai S., Weng J., Sui Y., Shi C., Huang Y., Chen S., Pan X., Fang X., Hu L., Kong F.and Wang K., *Sol. Energy Mater. Sol. Cells*, 2004, **84**, 125-133.

(97) Lee, W. J.; Ramasamy, E.; Lee, D. Y.; Song, J. S., *Sol. Energy Mater. Sol. Cells*, 2007, **91**, 1676-1680.

(98) Giordano, F.; Petrolati, E.; Brown, T. M.; Reale, A.; Di Carlo, A. *IEEE Transactions on Electron Devices*, 2011, **58**, 2759-2764.

(99) Mastroianni, S.; Lanuti, A.; Penna, S.; Reale, A.; Brown, T. M.; Di Carlo, A.; Decker, F. *ChemPhysChem*, 2012, **13**, 2925-2936.

(100) Hinsch, A.; Brandt, H.; Veurman, W.; Hemming, S.; Nittel, M.; Würfel, U.; Putyra, P.; Lang-Koetz, C.; Stabe, M.; Beucker, S.; Fichter, K., *Sol. Energy Mater. Sol. Cells*, 2009, **93**, 820-824.

(101) Ikegami, M.; Suzuki, J.; Teshima, K.; Kawaraya, M.; Miyasaka, T. *Sol. Energy Mater. Sol. Cells*, 2009, **93**, 836-839.

(102) Giordano, F.; Guidobaldi, A.; Petrolati, E.; Vesce, L.; Riccitelli, R.; Reale, A.; Brown, T. M.; Di Carlo, A. *Progr. Photovolt.: Res. Appl., Applications*, 2013, **21**, 1653-1658.

(103) Kato, N.; Takeda, Y.; Higuchi, K.; Takeichi, A.; Sudo, E.; Tanaka, H.; Motohiro, T.; Sano, T.; Toyoda, T. *Sol. Energy Mater. Sol. Cells*, 2009, **93**, 893-897.

(104) Wang, L.; Fang, X.; Zhang, Z., *Renew. Sust. Energ. Rev.*, 2010, **14**, 3178-3184.

(105) Kroon, J. M., Energy Research Center report, 2005, **ECN-C--05-078**, 1-41.

(106) Takeda, Y.; Kato, N.; Higuchi, K.; Takeichi, A.; Motohiro, T.; Fukumoto, S.; Sano, T.; Toyoda, T. *Sol. Energy Mater. Sol. Cells*, 2009, **93**, 808-811.

(107) Jun, Y.; Son, J.-H.; Sohn, D.; Kang, M. G. *J. Photochem. Photobiol.*, 2008, **200**, 314-317.

(108) Toyodaa, T. S., Nakajimaa J., Doia S., Fukumotoa S., Itoa A., Tohyamaa T., Yoshidaa M., Kanagawaa T., Motohirob T., Shigab T., Higuchib K., Tanakab H.,, Takedab H., Fukanob T., Katohb N., Takeichib A., Takechib K., Shiozawab M., . *Photochem. Photobiol.*, 2004, **164**, 203-207.

(109) Hopkins, J. A.; Phani, G.; Skryabin, I. L., Google Patents, 2006.

(110) Dai, S.; Weng, J.; Sui, Y.; Shi, C.; Huang, Y.; Chen, S.; Pan, X.; Fang, X.; Hu, L.; Kong, F.; Wang, K. *Sol. Energy Mater. Sol. Cells*, 2004, **84**, 125-133.

(111) Okada, K.; Matsui, H.; Kawashima, T.; Ezure, T.; Tanabe, N. *J. Photochem. Photobiol.*, 2004, **164**, 193-198.

(112) Kroon, J. M.; Bakker, N. J.; Smit, H. J. P.; Liska, P.; Thampi, K. R.; Wang, P.; Zakeeruddin, S. M.; Grätzel, M.; Hinsch, A.; Hore, S.; Würfel, U.; Sastrawan, R.; Durrant, J. R.; Palomares, E.; Pettersson, H.; Gruszecki, T.; Walter, J.; Skupien, K.; Tulloch, G. E. *Progr. Photovolt.: Res. Appl., Applications*, 2007, **15**, 1-18.

(113) Dai, S.; Weng, J.; Sui, Y.; Chen, S.; Xiao, S.; Huang, Y.; Kong, F.; Pan, X.; Hu, L.; Zhang, C.; Wang, K. *Inorg. Chim. Acta*, 2008, **361**, 786-791.

(114) Wei, T. C.; Lan, J. L.; Wan, C. C.; Hsu, W. C.; Chang, Y. H. *Prog. Photovolt: Res. Appl.*, 2012, **21**, 1625-1633.

(115) Kumara, G. R. A.; Kawasaki, S.; Jayaweera, P. V. V.; Premalal, E. V. A.; Kaneko, S. *Thin Solid Films*, 2012, **520**, 4119-4121.

(116) Takashima, J.; Fujii, T.; Furusaki, K., *Electrochem. Soc. meeting*, 2008, **MA2008-02**, 478.

(117) Zhang, Y. D.; Huang, X. M.; Gao, K. Y.; Yang, Y. Y.; Luo, Y. H.; Li, D. M.; Meng, Q. B. *Sol. Energy Mater. Sol. Cells*, 2011, **95**, 2564-2569.

(118) Pichot, F., Pitts, J. R., Gregg, B. A., *Langmuir*, 2000, **16**, 5626-5630.

(119) Kado, T., Yamaguchi, M., Yamada, Y. & Hayase, S. *Chem. Lett.*, 2003, **32**, 1056-1057.

(120) Fan, K.; Peng, T.; Chen, J.; Zhang, X.; Li, R. *J. Mater. Chem.*, 2012, **22**, 16121-16126.

(121) Fan, K.; Li, R.; Chen, J.; Shi, W.; Peng, T. *Sci. Adv. Mater.*, 2013, **5**, 1596-1626.

(122) Solaronix Webshop, http://shop.solaronix.com/electrode-materials.html,(accessed May 2014).

(123) Jen, H.-P.; Lin, M.-H.; Li, L.-L.; Wu, H.-P.; Huang, W.-K.; Cheng, P.-J.; Diau, E. W.-G., *ACS Appl. Mater. Inter.* 2013, **5**, 10098-10104.

(124) Jun, Y.; Kim, J.; Kang, M. G. *Sol. Energy Mater. Sol. Cells*, 2007, **91**, 779-784.

(125) L. Yang, U. B. Cappel, E. L. Unger, M. Karlsson, K. M. Karlsson, E. Gabrielsson, L. Sun, G. Boschloo, A. Hagfeldt and E. M. J. Johansson, *PCCP*, 2012, **14**, 779-789.

(126) H. C. Weerasinghe, F. Huang and Y.-B. Cheng, *Nano Energ.*, 2013, 2, 174-189.

(127) Macák J. M., Tsuchiya H., Schmuki P., *Angew. Chem. Int. Ed. Engl.*, 2005, **44**, 2100-2102.

(128) Grimes, C. A. *J. Mater. Chem.*., 2007, **17**, 1451-1457.

(129) Kuang D., Brillet J., Chen P., Takata M., Uchida S., Miura H., Sumioka K., Zakeeruddin S. M., Grätzel M., *ACS Nano*, 2008, **2**, 1113-1116.

(130) Dürr M., Schmid A., Obermaier, M., Rosselli S., Yasuda A., Nelles G., *Nature Mater.*, 2005, **4**, 607-611.

(131) Boschloo, G.; Lindström, H.; Magnusson, E.; Holmberg, A.; Hagfeldt, A. *J. Photochem. Photobiol.*, 2002, **148**, 11-15.

(132) M. Dürr, A. Yasuda and G. Nelles, *Appl. Phys. Lett.*, 2006, **89**.

(133) Yang, L.; Wu, L.; Wu, M.; Xin, G.; Lin, H.; Ma, T. *Electrochem. Comm.*, 2010, **12**, 1000-1003.

(134) Chen, H. W.; Lin, C. Y.; Lai, Y. H.; Chen, J. G.; Wang, C. C.; Hu, C. W.; Hsu, C. Y.; Vittal, R.; Ho, K. C. *J. Pow. Sources*, 2011, **196**, 4859-4864.

(135) Senthilarasu, S., Peiris, T. A. N., García-Cañadas, J., Wijayantha, K. G. U., *J. Phys. Chem. C*, 2012, **116**, 19053-19061.

(136) Zhang D., Yoshida T., Oekermann T., Furuta K., Minoura H., *Adv. Funct. Mater.*, 2006, **16**, 1228-1234.

(137) Vesce L., Riccitelli R., Soscia G., Brown T. M., Di Carlo A., Reale A., *J. Non-Cryst. Solids,* 2010, **356,** 1958-1961.

(138) Lee S. W., *Mol Cryst Liquid Cryst.,* 2011, **551**, 172-180.

(139) Noh, S. I.; Bae, K. N.; Ahn, H. J.; Seong, T. Y. *Ceram. Int.,* 2013, **39**, 8097-8101.

(140) Wu, J.; Xiao, Y.; Tang, Q.; Yue, G.; Lin, J.; Huang, M.; Huang, Y.; Fan, L.; Lan, Z.; Yin, S.; Sato, T. *Adv. Mater.* 2012, **24**, 1884-1888.

(141) Biancardo, M.; West, K.; Krebs, F. C. *Sol. Energy Mater. Sol. Cells,* 2006, **90**, 2575-2588.

(142) Nei de Freitas, J.; Longo, C.; Nogueira, A. F.; De Paoli, M.-A., *Sol. Energy Mater. Sol. Cells,* 2008, **92**, 1110-1114.

(143) Hinsch, A.; Veurman, W.; Brandt, H.; Loayza Aguirre, R.; Bialecka, K.; Flarup Jensen, K. *Prog. Photovolt: Res. Appl.,* 2012, **20**, 698-710.

(144) Liu, Y.; Wang, H.; Shen, H.; Chen, W. *Appl. Energy*, 2010, **87**, 436-441.

(145) Wei, T. C.; Feng, S. P.; Chang, Y. H.; Cherng, S. J.; Lin, Y. J.; Chen, C. M.; Chen, H. H., *Int. J. Electrochem. Sci.* 2012, **7**, 11904-11916.

(146) Sastrawan R., Renz J., Prahl C., Beier J., Hinsch A. and Kern R., *J. Photochem. Photobiol. A,* 2006, **178**, 33-40.

(147) Cornaro, C.; Bartocci, S.; Musella, D.; Strati, C.; Lanuti, A.; Mastroianni, S.; Penna, S.; Guidobaldi, A.; Giordano, F.; Petrolati, E.; Brown, T. M.; Reale, A.; Di Carlo, A. *Prog. Photovolt: Res. Appl.,* 2013.

(148) Yella, A.; Lee, H.-W.; Tsao, H. N.; Yi, C.; Chandiran, A. K.; Nazeeruddin, M. K.; Diau, E. W.-G.; Yeh, C.-Y.; Zakeeruddin, S. M.; Grätzel, M. *Science,* 2011, **334**, 629-634.

(149) Chiba, Y.; Islam, A.; Watanabe, Y.; Komiya, R.; Koide, N.; Han, L. *Jap. J. App. Phys.* 2006, **45**, L638-L640.

(150) Schiefer, S.; Zimmermann, B.; Würfel, U. *Sol. Energy Mater. Sol. Cells*, 2013, **115**, 29-35.

(151) I. Chung, B. Lee, J. He, R. P. H. Chang and M. G. Kanatzidis, *Nature*, 2012, 485, 486-489.

(152) Wei, T. C.; Lan, J. L.; Wan, C. C.; Hsu, W. C.; Chang, Y. H. *Prog. Photovolt: Res. Appl.,* 2013, **21**, 1625-1633.

(153) Fakharuddin, A.; Archana, P. S.; Kalidin, Z.; Yusoff, M. M.; Jose, R. *RSC Adv.* 2013, **3**, 2683-2689.

(154) Jose, R.; Fakharuddin, A.; Archana, P. S.; Yusoff, M. M., *Ab. Am. Chem. Soc.,* American Chemical Society spring meeting, New Orleans USA, **245**, 2013.

(155) A. Fakharuddin; I. Ahmed; Z. Khalidin; M. M. Yusoff; Jose R., *App. Phy. Lett.* 2014, **104**, 053905.

(156) Fakharuddin, A.; Ahmed, I.; Khalidin, Z.; Yusoff, M. M.; Jose, R., *J. Appl. Phys.* 2014, **115**, 164509.

(157) Fakharuddin, A.; Ahmed, I. Wali Q.; Khalidin, Z.; Yusoff, M. M.; Jose, R., *Adv. Mater. Res.,* 2014, **295**, 553-558.

(158) Nelson, J. *Phys. Rev. B* 1999, **59**, 15374-15380.

(159) Bisquert, J. *J. Phys. Chem. C,* 2007, **111**, 17163-17168.

(160) Gonzalez-Vazquez, J. P.; Anta, J. A.; Bisquert, J. *PCCP*, 2009, **11**, 10359-10367.

(161) Martinson, A. B. F.; Góes, M. r. S.; Fabregat-Santiago, F.; Bisquert, J.; Pellin, M. J.; Hupp, J. T. *J. Phys. Chem. A*, 2009, **113**, 4015-4021.

(162) Gagliardi, A.; Gentilini, D.; Carlo, A. D *J. Phys. Chem. C*, 2012, **116**, 23882-23889.

(163) Nelson, G. J.; Cassenti, B. N.; Peracchio, A. A.; Chiu, W. K. S. *Electrochim. Acta*, 2013, **90**, 475-481.

(164) Jennings, J. R.; Peter, L. M. *J. Phys.Chem. C*, 2007, **111**, 16100-16104.

(165) Gonzalez-Vazquez, J. P.; Anta, J. A.; Bisquert, J. *J. Phys. Chem. C*, 2010, **114**, 8552-8558

(166) Navas, J.; Guillén, E.; Alcántara, R.; Fernández-Lorenzo, C.; Martín-Calleja, J.; Oskam, G.; Idígoras, J.; Berger, T.; Anta, J. A. *J.Phys. Chem. L.*, 2011, **2**, 1045-1050.

(167) Fabregat-Santiago, F.; Bisquert, J.; Palomares, E.; Otero, L.; Kuang, D.; Zakeeruddin, S. M.; Grätzel, M. *J. Phys. Chem. C*, 2007, **111**, 6550-6560.

(168) Sommeling, P. M. K., J.M., 24th European Photovoltaic Solar Energy Conference and Exhibition, Hamburg, Germany, 2009.

(169) Asghar, M. I.; Miettunen, K.; Halme, J.; Vahermaa, P.; Toivola, M.; Aitola, K.; Lund, P. *Energ. Environm. Sci.*, 2010, **3**, 418-426.

(170) Kern R., N. v. d. B., G. Chmiel, J Ferber, G. Hasenhindl, A. Hinsch, R. Kinderman,J.M. Kroon, A. Meyer, T. Meyer, R. Niepmann, J.A.M. van Roosmalen, C. Schill, P. Sommeling, M. Späth , I. Uhlendorf, *Optoelectron. Rev.* 2000, **8**, 284-288.

(171) J.M. Kroon, A. H., J.A.M. van Roosmalen, N.P.G. van der Burg, N.J. Bakker, R. Kinderman, P.M. Sommeling, M. Späth, R. Kern, R. Sastrawan, J. Ferber, M. Schubert, G. Hasenhindl, C. Schill, M. Lorenz, R. Stangl, S. Baumgärtner, C. Peter, A. Meyer, T. Meyer, I. Uhlendorf, J. Holzbock, Regine Niepmann, *Energy Research Center report*, 2001, **JOR3-CT98-0261**, 1-11.

(172) Peng Wang, C. K., Robin Humphry-Baker, Shaik M. Zakeeruddin, and Michael Grätzel *App. Phy. Lett.*, 2005, **86**, 123508.

(173) P. Wang, S. M. Z., J.-E. Moser, M. K. Nazeeruddin, T. Sekiguchi, and M. Grätzel *Nat. Mater.*, 2003, **2**, 402.

(174) P. Wang, S. M. Z., R. Humphry-Baker, J.-E. Moser, and M. Grätzel *Adv. Mater.*, 2003, **15**, 2101.

(175) B. Macht, M. Turrión, A. Barkschat, P. Salvador, K. Ellmer and H. Tributsch, *Sol. Energy Mater. Sol. Cells*, 2002, **73**, 163-173.

(176) S. Mastroianni, I. Asghar, K. Miettunen, J. Halme, A. Lanuti, T. M. Brown and P. Lund, *PCCP*, 2014, **16**, 6092-6100.

(177) H. B. K. F. Jensen, C. Im, J. Wilde, A. Hinsch, presented in part at the 28th European PV Solar Energy Conference and Exhibition, Paris, France, 2013.

(178) A. G. Kontos, T. Stergiopoulos, V. Likodimos, D. Milliken, H. Desilvesto, G. Tulloch and P. Falaras, *J. Phys. Chem. C*, 2013, 117, 8636-8646.

(179) Kroon J.M., P. M. S., N.J. Bakker, H. van Mansom, A. Hinsch, W. Veurman, H. Pettersson, T. Gruszecki, B.C. O'Regan, F. Sauvage, S.M. Zakeeruddin, M. Grätzel, E. Palomares, J. Clifford, E. Martínez, T. Torres, M. Feigenson, B. Breen, S. Vallon, S. Logunov, M. Spratt, *25th European Photovoltaic Solar Energy Conference and Exhibition*: Valencia, Spain, 2010, pp 306-311.

(180) Lee K.-M., C.-Y. Chen, Y.-T. Tsai, L.-C. Lin and C.-G. Wu, *RSC Adv.*, 2013, 3, 9994-10000.

(181) Goldstein J., Yakupov I. and Breen B., *Sol. Energy Mater. Sol. Cells*, 2010, **94**, 638-641.

(182) Wang X., Deng R., Kulkarni S. A., Wang X., Pramana S. S., Wong C. C., Gratzel M., Uchida S. and Mhaisalkar S. G., *J. Mater. Chem. A*, 2013, **1**, 4345-4351.

(183) Mastroianni S., Lembo A., Brown T. M., Reale A. and Di Carlo A., *ChemPhysChem*, 2012, **13**, 2964-2975.

(184) S. Mastroianni, A. Lanuti, T. M. Brown, R. Argazzi, S. Caramori, A. Reale and A. Di Carlo, *Appl. Phys. Lett.*, 2012, **101**.

(185) Hirnori Arakawa T. Y., Okada K., Masturi H., Kitamura T., Tanabe N., *Vol. Fujikura Technical Reviews, 2009, pp.* 55-60.

(186) C. B. Claudia Barolo, Rita Boaretto, Thomas Brown, Luca Bonandini, Eva Busatto, Stefano Caramori, Daniele Colonna, Gabriele De Angelis, Aldo Di Carlo, Alessandro Guglielmotti, and A. L. Andrea Guidobaldi, Angelo Lembo, Daniele Magistri, Valentina Mirruzzo, Stefano Penna, Serena Pietrantoni, Donato Prencipe, Andrea Reale, Riccardo Riccitelli, Alessandra Smarra, Giuseppe Soscia, Roberto Tagliaferro, Luigi Vesce, Guido Viscardi, Paolo Mariani, , proceeding of HOPV14, page 72. 2014.

(187) Yang, X.; Yanagida, M.; Han, L. *Energ. Environmen. Sci.* 2013, **6**, 54-66.

(188) L. Tillemann, *http://energy.gov/sites/prod/files/2013/09/f2/200130917-revolution-now.pdf U.S. DEPARTMENT OF ENERGY*, 2013.

(189) H. Zervos, *http://www.idtechex.com/research/reports/dye-sensitized-solar-cellsdssc-dsc-2013-2023-technologies-markets-players-000345.asp?viewopt%BCshowall&viewopt=contents* , ID-TechEx, 2013.

(190) S. Yoon, S. Tak, J. Kim, Y. Jun, K. Kang and J. Park, *Build. Environ.*, 2011, 46, 1899-1904.

(191) A. Reale, L. Cinà, A. Malatesta, R. De Marco, T. M. Brown and A. Di Carlo, *Energ. Tech.*, 2014, 2, 531-541.

TOC entry

An overview of the state of the art dye solar module technology and innovations required for further development is presented.